

UNIVERSITY OF CALIFORNIA  
**MERCED**

---

# Thunder\_Cats AIAA Design/Build/Fly

## 2019 Design Report



## Contents

<b>1</b>	<b>Executive Summary</b>	<b>1</b>
<b>2</b>	<b>Management Summary</b>	<b>2</b>
2.1	Team Organization . . . . .	3
2.2	Milestone Chart . . . . .	3
<b>3</b>	<b>Conceptual Design</b>	<b>4</b>
3.1	Mission Requirements . . . . .	4
3.1.1	Scoring Summary . . . . .	5
3.1.2	Pre-Mission Requirements . . . . .	5
3.1.3	Mission 1: Demonstration Flight . . . . .	5
3.1.4	Mission 2: Reconnaissance Mission . . . . .	6
3.1.5	Mission 3: Attack Mission . . . . .	6
3.1.6	Ground Mission . . . . .	6
3.1.7	Aircraft Constraints . . . . .	7
3.2	Design Requirements . . . . .	8
3.2.1	Flight Score Sensitivity & Aircraft Performance Analysis . . . . .	8
3.2.2	Ground Mission Analysis . . . . .	10
3.3	Configuration Selection . . . . .	10
3.3.1	Configurations Considered . . . . .	10
3.3.2	Configurations Selection Process . . . . .	12
3.4	Configuration Optimization For Mission Requirements . . . . .	13
3.4.1	Wing Configuration . . . . .	14
3.4.2	Wing Packaging Approach . . . . .	14
3.4.3	Tail Configuration . . . . .	15
3.4.4	Attack Store Configuration . . . . .	16
3.4.5	Radome Configuration . . . . .	17
3.5	Final Conceptual Design . . . . .	18
<b>4</b>	<b>Preliminary Design</b>	<b>19</b>
4.1	Design Methodology . . . . .	19
4.2	DTS_Cat . . . . .	20
4.3	Design Trade Studies . . . . .	23
4.3.1	Wing Geometry . . . . .	23
4.3.2	Propulsion System Sizing . . . . .	24
4.4	Mission Model . . . . .	25
4.5	Aerodynamics . . . . .	26
4.5.1	Airfoil Selection . . . . .	26
4.5.2	Drag Analysis . . . . .	27
4.6	Stability and Control . . . . .	28
4.6.1	Static Stability . . . . .	28
4.6.2	Dynamic Stability . . . . .	29
4.7	Transitioning to Stowed Configuration . . . . .	29
4.8	Performance Estimates . . . . .	31

<b>5 Detail Design</b>	<b>31</b>
5.1 Dimensional Parameters Table . . . . .	31
5.2 Structural Characteristics and Capabilities . . . . .	32
5.2.1 Fuselage and Frame . . . . .	32
5.2.2 Wing . . . . .	33
5.2.3 Tail . . . . .	34
5.3 Subsystem Design and Integration Architecture . . . . .	34
5.3.1 Pivot Wing Mechanism . . . . .	34
5.3.2 Attack Stores . . . . .	34
5.3.3 Plug in Radome . . . . .	35
5.3.4 Electronics Bay . . . . .	36
5.3.5 Propulsion System . . . . .	36
5.3.6 Landing Gear . . . . .	37
5.4 Weight and Mass Balance . . . . .	38
5.5 Flight and Mission Performance . . . . .	39
5.6 Drawing Package . . . . .	39
<b>6 Manufacturing Plan and Process</b>	<b>40</b>
6.1 Manufacturing Methods Considered . . . . .	40
6.2 Manufacturing Process Selected . . . . .	40
6.3 Manufacturing Milestone Chart: . . . . .	42
<b>7 Testing Plan</b>	<b>42</b>
7.1 Test Objectives . . . . .	43
7.2 Subsystem Testing . . . . .	43
7.2.1 Propulsion Testing . . . . .	43
7.2.2 Structural Testing . . . . .	44
7.2.3 Subsystem Testing: Radome . . . . .	44
7.2.4 Subsystem Testing: Attack Stores . . . . .	44
7.2.5 Takeoff Ramp Testing . . . . .	45
7.3 Flight Test Schedule and Plan . . . . .	45
7.4 Flight Checklists . . . . .	46
<b>8 Performance Results</b>	<b>47</b>
8.1 Demonstrated Performance of Key Subsystems . . . . .	47
8.2 Demonstrated Flight Performance of Aircraft . . . . .	48

## Acknowledgements

### **Mr. Reuben Garcia, Technical Director for Masten Space Systems:**

We would like to thank Mr. Reuben Garcia, the Technical Director for Masten Space Systems, for his generous materials donation and composites training. With his mentorship and guidance, the team was able to quickly develop its composite manufacturing skills that further advanced manufacturing capabilities allowing us to materialize complex designs that met or exceeded design specifications.

### **Dr. YangQuan Chen, MESA Lab Founder and Director, Faculty Advisor at UCM:**

We would also like to thank our faculty advisor Dr. YangQuan Chen for continually supporting all efforts of our AIAA UCM Branch, by providing us with the necessary workspace and guidance to conduct our chapter business. Without the continual support of Dr. YangQuan Chen, the aerospace passion of UCM students would not have had the opportunity to flourish and develop.

### **Derek Hollenbeck, Graduate Student Advisor at UCM:**

We would also like to thank Derek Hollenbeck, graduate student of Dr. YangQuan Chen and past UCM Design/Build/Fly project manager for his continuous support, encouragement, and technical insight for our project and its development.

## Nomenclature

Thunder_Cats	UCM DBF Team Name	$Drag_{wing}$	Force of Drag Introduced by the Wing
CG	Center of Gravity	$Height_{wing}$	Thickness of Airfoil
CF	Carbon Fiber	$Drag_{fuselage}$	Force of Drag Introduced by the Fuselage
DTS_Cat	MATLAB tool for Modeling Flight	$Drag_{tail}$	Force of Drag Introduced by the Tail
UCM	University of California, Merced	$Drag_{ATK}$	Force of Drag Introduced by the Attack Stores
Kirin	Name of Thunder_Cats Plane	$Cd_{wing}$	Coefficient of Drag of Wing Airfoil
DBF	Design/Build/Fly	$Cd_{fuselage}$	Coefficient of Drag of Fuselage
AIAA	American Institute of Aeronautics and Astronautics	$CSA_{fuselage}$	Cross Sectional Area of Fuselage
$M_1$	Mission 1 Flight Score	$Cd_{TVS}$	Coefficient of Drag of Tail Vertical Stabilizer Airfoil
$M_2$	Mission 2 Flight Score	$L_{TVS}$	Length of Tail Vertical Stabilizer
$M_3$	Mission 3 Flight Score	$Height_{TVS}$	Thickest Measure of Tail Vertical Stabilizer
$GM$	Ground Mission Flight Score	$Cd_{THS}$	Coefficient of Drag of Tail Horizontal Stabilizer Airfoil
$min_{M_2time}$	Fastest completion time for mission 2	$L_{THS}$	Length of Tail Horizontal Stabilizer
$N_{time}$	UCM time for mission 2	$Height_{THS}$	Thickest Measure of Tail Horizontal Stabilizer
$N_{stores}$	Number of Attack Stores to be Dropped	$Cd_{attackstore}$	Coefficient of Drag of Attack Store
$min_{GMtime}$	Fastest completion time for mission 2	$A_{attackstore}$	Cross Sectional Area of Attack Store
NiCd	Nickel-Cadmium Batteries	$P_{req}$	Power Required by Battery to Cruise at $v$
NiMH	NNickel-Metal Hydride Batteries	$P_{batt}$	Power of One Battery
Acc	Acceleration of Plane from a Standstill	$CHK_{takeoff}$	Algorithmic Validation of Model to Takeoff
$Min_{speed}$	Stall Speed at 10° Attack	$CHK_{laps}$	Algorithmic Validation of Model to Complete $N_{store}$ Laps
$Width_{stow}$	Width of Plane in the Stowed Position	ESC	Electronic Speed Controller
AR	Aspect Ratio	CFRP	Carbon Fiber Reinforced Polymer
FoM	Figures of Merit	GFRP	Glass Fiber Reinforced Polymer
$F_l$	Force of Lift	TMS	Total Mission Score
$F_t$	Force of Thrust	WAM	Wing Actuation Mechanism
$W_{plane}$	Weight of Empty Plane	CA	cyanooacrylate
$W_{total}$	Wight of completely equipped plane	PLA	polylactic acid
$W_{store}$	Weight of One Attack Store		
$W_{batt}$	Weight of One Battery		
$N_{batts}$	Number of Batteries		
$\rho_{ho}$	Density of Air Based On Arizona's April Climate History		
$v$	Velocity of Plane		
$L_{ws}$	Total Length of Wing Airfoil (Wingspan)		
$L_{wc}$	Length of Wing Chord		
$Cl$	Coefficient of Lift		

## 1 Executive Summary

The objective of team Thunder\_Cats is to design a multi-purpose aircraft that supports carrier operations, able to launch within 10 ft on a 4 ft wide by 10 ft long ramp angled at an incline of approximately 5 degrees. The aircraft must also be capable of self-transitioning and self-locking from stowed configuration to flight configuration, via pilot command prior to completing three launched flight missions in Tucson, Arizona. In addition, the aircraft must meet the full requirements and design necessities of the 2019 DBF rules. At the time of writing, over six flight tests have been performed on the aircraft.

The first flight mission, a demonstration flight, consists of flying three laps with no payload in five minutes or less. The second flight mission, a reconnaissance mission, requires the plane to have a selectively rotating radome as a payload and complete three laps within five minutes. The third flight mission, an attack flight, requires the aircraft to carry and deploy the maximum amount of attack stores; only one attack store may be dropped per lap, and the mission must be completed within 10 minutes. The ground mission, a timed assembly mission, requires a crew member and pilot to be present with the aircraft in a 10 ft by 10 ft mission box. The assembly crew member is the only person able to directly interact with the aircraft and the pilot is responsible for remote payload operation. The ground mission score directly affects the overall score and is a function of how fast payload can be loaded, indicating that keen optimization must be made in how payload configurations are loaded.

Once completing the flight mission scoring and performance analysis, the team determined that the amount of attack stores the aircraft would be able to carry is constrained to (1) the 10 foot take off ramp limitation with a 5 degree incline, (2) the CG shift of the aircraft with no payload in the stowed configuration, and (3) the power that the propulsion system is able to safely output for all missions. Further performance trade studies indicated that given the limitations of take-off distance and propulsion output, the highest attack store payload number achievable is 8-12, due to constraints (1), (2), and (3).

A Diamond Drop configuration was designed and selected due to key strategic advantages compared to other commonly available configurations. One advantage was that it allowed weight reduction while simultaneously giving the pilot more roll authority in the air to offset the characteristics of the strongly stable design. Wing and tail loads are transferred to key loading components in the fuselage fabricated out of carbon fiber, (A) a light weight wing mounted coupler doubling as the center piece of the fuselage to provide lateral stability, and (B) a thick CF rod extending throughout the plane mounted to (A). A centralized loading structure allowed the majority of the plane to be composed of lighter materials such as balsa or high-density polystyrene foam. A vertically offset conventional design was selected as the empennage configuration to address the flow complexities that the radome and the wing introduce. The geometry of the aircraft flight surfaces was first sized quantitatively using DTS\_Cat and then validated experimentally by extensive ramp launch testing that simulate flight conditions in mission 1, mission 2, and mission 3. All mission payloads are fully serviceable and are mounted on the CG point to prevent any contribution to the longitudinal stability characteristics of the plane.

The University of California, Merced's aircraft, Kirin, is designed to maximize score by combining variable-speed flight performance, high lift characteristics, high payload capabilities, and innovative subsystem architectures that resulted in a sleek compact design with flight characteristics of a larger aircraft. Kirin takes off at 24 ft/s and quickly climbs to cruise altitude and velocity for all missions at 100 ft and 65 ft/s-100 ft/s respectively. Kirin will complete mission 1 at flight speed 80 ft/s, having a total weight of 3.3 lbs, within 2.8 minutes. Kirin will complete mission 2 at flight speed 100 ft/s with a total weight of 3.5 lbs, within 2.5 minutes. Kirin completes mission 3 at a variable flight speed of 65-95 ft/s with a total weight of 5.9 pounds, successfully engaging 12 (Max) attack stores, one each lap within 9.2 minutes. Kirin appears to be a mid-wing aircraft, however the Diamond Drop design localizes all nonstructural mass below the center of lift, effectively making the aircraft behave similar to a high-wing configuration. The upper portion of the fuselage serves an aerodynamic purpose and as extra payload capacity if needed.



Figure 1.0.1: 2019 UC Merced Design/Build/Fly Competition Plane, Kirin

## 2 Management Summary

The 2018-2019 University of California, Merced (UCM) Design/Build/Fly (DBF) team, Thunder\_Cats, consists of 18 students that participate on an extracurricular basis. Nine team members are seniors and the remainder are juniors and underclassmen. The team is entirely student-led, but receives guidance and technical support when needed from industry advisers, two academic advisers, one graduate student advisor, and the team's aeronautical chair. The team also holds weekly meetings to build and design; other meetings are held to plan expected due dates for project goals, and for all team members to discuss ideas and steps to achieve the set goals. In addition the team is divided into synergistic engineering teams, which all communicate and work together to optimize efficiency and effectiveness for all stages of the competition. Members were assigned to the following sub-teams: design engineers, aerodynamics and systems/controls engineers, manufacturing engineers, electronics engineers, and flight engineers. Team assignments were made by the recommendations of project managers, based on a member's previous experience in DBF, leadership skills, knowledge of the sub-team tasks, and

specific skills and interests of each member. It is important to note that the teams were made so that everyone had a primary task but members worked and were encouraged to help other team members and therefore overall production.

## 2.1 Team Organization

For 2019, DBF organization was restructured to better reward motivation, passion, and promote quick learning and application of newly gathered knowledge. Despite there being no aeronautical program at UCM and the majority of the 2019 UCM DBF students having junior level or below class standing with no previous aircraft modelling experience, the restructuring resulted in a much-improved productivity output in comparison with previous years. The revision includes (1) the introduction of the agile method, creating an iterative approach to the project planning and execution processes, and (2) the addition of an optimization team to vet design decisions. Figure 2.1.1 depicts the team structure as previously mentioned. In order to help with productivity, individual learning, and communication team members were invited to work in multiple areas, developing their skills in a multidisciplinary fashion.

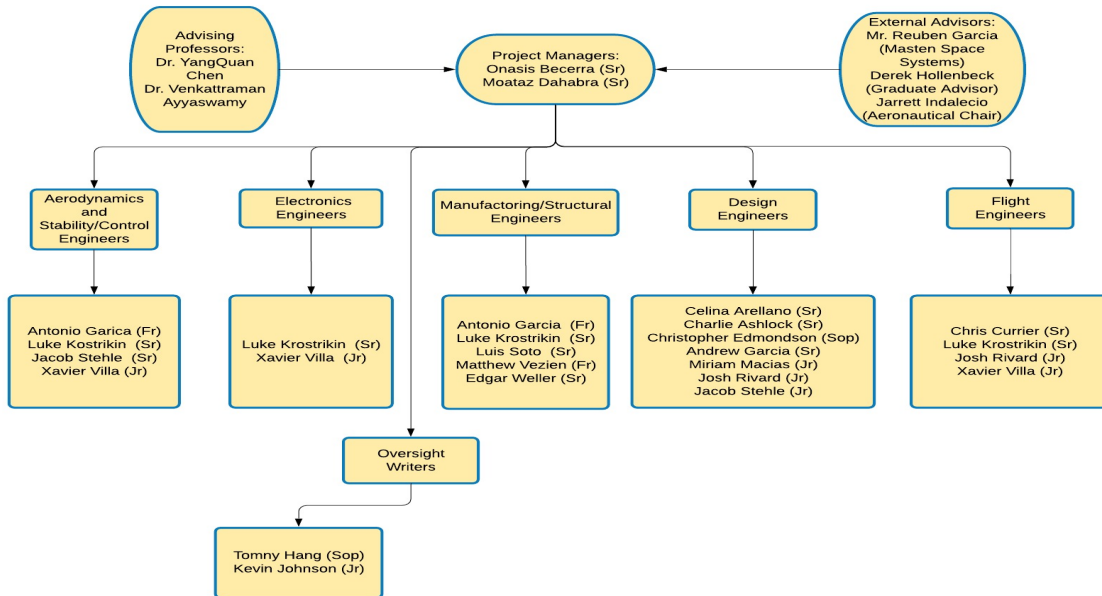


Figure 2.1.1: UC Merced Team Organization Chart

## 2.2 Milestone Chart

At the beginning of the competition, a milestone chart, shown in figure 2.2.1, was established to ensure that major deadlines for each engineering team were met. Weekly logistical meetings occurred to help plan and establish build day meetings, prevent the team from falling behind schedule, and ensuring there was little to no miscommunication. Within the milestone chart, tasks and major deadlines are organized by actual and projected dates. Actual timing is not shown for future tasks.

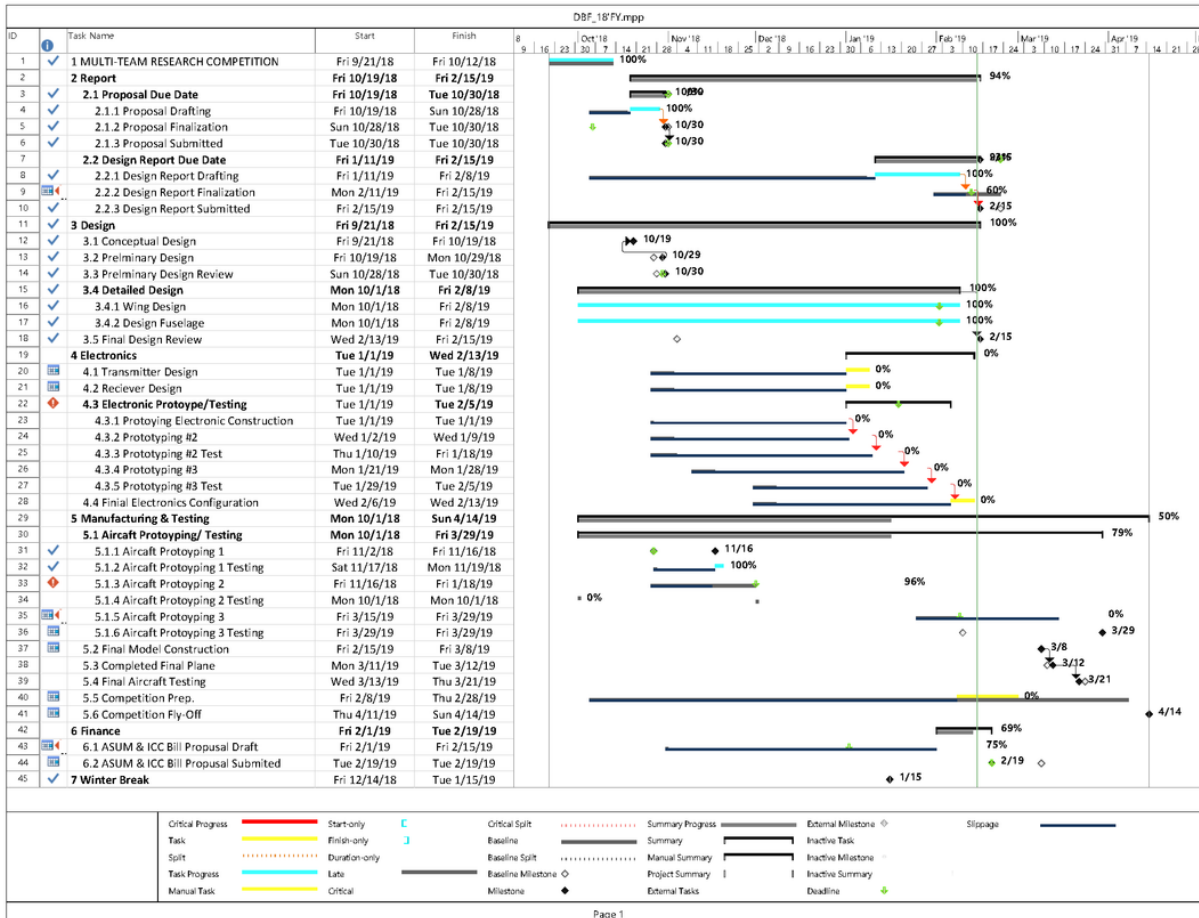


Figure 2.2.1: Team Gantt Chart

## 3 Conceptual Design

### 3.1 Mission Requirements

This year's rules for the 2018-2019 American Institute of Aeronautics and Astronautics (AIAA) DBF competition tasks teams to design a multi-purpose aircraft that supports carrier operations. To be able to complete the ground and mission's one, two, and three, the team is expected to follow general guidelines. The aircraft is expected to have a minimum wingspan of four ft, while having folding wings that can fit in a 3ft x 2ft box while in its stowed configuration. In addition, the nose of the aircraft and all the landing gear is expected to fit within a depth of two ft of the box. Lastly, the aircraft is expected to transition from the stowed condition, to flight readiness remotely from the transmitter and to mechanically lock without any external assistance.

This year's competition requires that for all three missions takeoff is from a launch ramp that is 4 ft wide by 10 ft long and at a launch angle of approximately 5 degrees. The aircraft will start from the low end of the ramp and must not touch the ground from the high end of it. Also, the aircraft must have a tail hook, located and centered in

the bottom of the fuselage. The tail hook, must be designed to restrain during power up and release at take-off. The flight missions require the aircraft to initiate take off from the start line, and perform the expected laps of two 1000 ft straightaways, two 180° turns, and a 360° turn opposite to flight and return to its original path. Figure 3.1.1 serves a clear schematic of the competition lap.

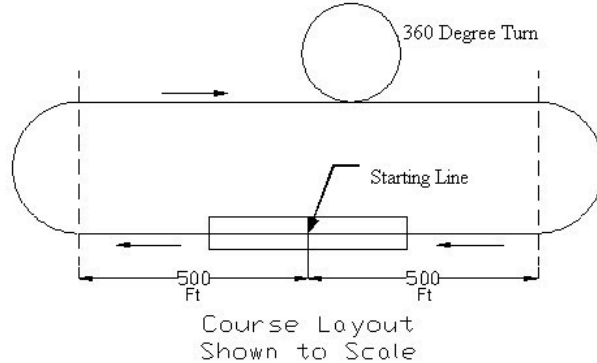


Figure 3.1.1: AIAA Competition Mission Layout

### **3.1.1 Scoring Summary**

The overall score for the 2019 AIAA DBF competition given by Eq. 1

$$\text{Score} = \text{Written Report Score} \times \text{Total Mission Score} \quad (1)$$

The written report score is based on the quality of the design report, while the total mission score is a sum of each mission as seen in Eq. 2.

$$\text{Total Mission Score} = M_1 + M_2 + M_3 + GM \quad (2)$$

$M_1$ ,  $M_2$ ,  $M_3$ , and  $GM$  denote the scores from the three flight missions, and the ground mission respectively.

### **3.1.2 Pre-Mission Requirements**

Prior to any missions the aircraft must undergo technical and safety inspections. The aircraft will begin tech inspection in the stowed/ neutral configuration, and upon instruction it will be remotely commanded into flight configuration. The self locking mechanism, electronic wiring, and safety features will be inspected and verified. Once that is complete, the team will install the radome and demonstrate the method of remotely actuating rotation. After that, the team will load the maximum number of stores for mission 3 and the aircraft will undergo a wing tip load test in this configuration. The maximum load demonstrated will be recorded and can not be changed. In addition all battery packs intended to be used in the competition will be inspected.

### **3.1.3 Mission 1: Demonstration Flight**

The objective of Mission 1 is to take off from the ramp and complete three laps within the prescribed 5 minute flight window without attack stores or radome attached; landing is not considered as part of the time window. The time for the mission only starts when the tail hook of the plane position on the ramp is released by a ground crew

member. Time only stops after the aircraft crosses the start/finish line. The scoring is shown in Eq. 3.

$$M_1 = 1.0 \text{ for successful mission.} \quad (3)$$

### **3.1.4 Mission 2: Reconnaissance Mission**

The objective of mission 2 is to take off from the ramp to perform 3 laps with the radome attached to the aircraft within a 5 minute flight window. The flight windows starts the moment the ground crew member releases the plane's tail hook. After the plane completes its first 180 degree turn the plane proceeds to spin its radome. There will be a visual indicator so that it will be obvious when the radome is in motion. The radome continuous spinning until the final 180 degree turn on the final lap where it stops spinning. The time only stops once the plane crosses the start/finish line at the end of the third lap. The landing is not counted in the flight window time, the landing must be successful for points to be attributed to the team according to the Eq. 4.

$$M_2 = 1 + [Min_{time}/N_{time}] \text{ Where } Min_{time} \text{ is the fastest time for 3 laps of all teams} \quad (4)$$

### **3.1.5 Mission 3: Attack Mission**

The objective of mission 3 is to complete as many scoring laps as possible within the flight window of 10 minutes. A scoring lap is where the aircraft completes a lap by crossing over the start/finish line and only drops one attack store by remote. The flight window time starts when the plane's tail hook is released by a ground crew member. The Time only stops when the plane crosses over the start/finish line after the final lap. A successful landing is required for all points to count, landing doesn't count towards the flight window time. The score for this mission is calculated by Eq. 5.

$$M_3 = 2 + N_{stores} \text{ Where } N_{stores} \text{ is the number of scoring laps} \quad (5)$$

### **3.1.6 Ground Mission**

The objective of the ground mission is a ground demonstration of missions 2 and 3. Where by the mission will begin with the aircraft inside of a 10ft x 10ft mission box. Where a team consisting of assembly crew member and the pilot are first tasked with the installation of the radome. When the official states go the time starts and the aircraft is commanded to flight configuration. After which the radome is attached to the plane time stops when the assembly crew crosses the start/finish line. At which point the pilot will demonstrate the radome's functionality. After this the official will say, "go" again where the time resumes and the assembly crew member will attach 4 attack stores to the aircraft. Time stops when the assembly crew member crosses the start/finish line. Once this has been completed the aircraft will be armed and the flight controls will be tested. In addition the attack store mechanism will be tested where one store will be dropped one at a time. Once this has been completed the mission is completed and score will be calculated with Eq. 6.

$$GM = [Min_{time}/N_{time}] \text{ Where } Min_{time} \text{ is the fastest time for all teams} \quad (6)$$

### 3.1.7 Aircraft Constraints

In addition to the flight missions characterized above, all aircraft must adhere to the following constraints specified by the 2019 competition rules:

- General
  - The aircraft may be of any configuration except rotary wing or lighter-than-air.
  - No structure or components may be dropped from the aircraft during flight other than one attack store per lap during mission 3.
  - The minimum wingspan of the aircraft is 4 ft.
- Stowed Configuration
  - The aircraft must have folding surfaces such that it will fit within a 3 foot wide, 2 foot high box.
  - The nose and all landing gear must fit in the box within a depth of 2 ft.
  - The aircraft must be able to roll completely through the 3ft x 2ft x 2ft box without any interference.
  - The aircraft must transition from the stowed configuration to the flight configuration remotely and mechanically lock without any assistance.
- Propulsion System
  - Batteries must be Nickel-Cadmium (NiCd) or Nickel-Metal Hydride (NiMH).
  - Must be propeller driven and electric powered with an unmodified over-the-counter model electric motor. May use multiple motors and/or propellers.
  - For safety, the aircraft must have an externally accessible switch to turn on the radio control system. It cannot be internal or under a panel or hatch.
  - The propulsion battery pack must power propulsion systems only, radio receivers and servos must be on a separate battery pack.
- Rotating Radome
  - The radome must be solid and circular in platform
  - The radome has a mandatory 12 inch minimum diameter and 1 inch minimum thickness in the center.
  - The radome is mounted on the aircraft center line.
  - There is a minimum clearance of 3 inches between any part of the radome and any surface of the aircraft except for the mounting structure/post.
  - The radome must be able to start and stop rotating on command during flight. Rotation needs to be clearly visible to flight line judges.
- Attack Store Payload
  - The aircraft must carry a minimum of four stores under the wing. Others may be located elsewhere
  - A minimum of 0.5 inch clearance is needed between stores and any part of the aircraft except for mounting hardware.
  - All stores need to be capable of remote detachment/separation individually and independently

- Ramp Take Off
  - For each flight mission the aircraft will take off from a 4ft x 10ft launch ramp with an angle of 5 degrees.
  - The low end of the ramp will be the starting point for takeoff with all landing gear on the ramp.
  - The aircraft must have a tail hook on the bottom center line of the fuselage of sufficient length, size, and strength such that the ground crew member can hold the tail hook for restraint during power up and release for take-off.

## 3.2 Design Requirements

The first round of the minimum design requirements were set by DBF rules. Immediately after these requirements were fully understood, analysis began on the DBF scoring rubric provided for the competition. Upon analyzing the scoring rubric, the most sensitive variables were regarded with the highest merit. All subsequent design requirements were chosen in order to maximize score by biasing variables with higher merit. Minimum mission requirements and score optimization equations are translated into design requirements in table 3.2.1.

Requirement	Objective	Parameter
10 ft takeoff (up ramp)	Maximize ratio of acceleration to stall speed	$Acc/Min_{speed}$
Folding wing mechanism	2 Foot stow width	$W_{stow}$
Attack store mechanism	Drop a minimum of 4 attack stores	$N_{stores}$

Table 3.2.1: Design Parameters Translated from Mission Requirements

### 3.2.1 Flight Score Sensitivity & Aircraft Performance Analysis

Analyzing the DBF scoring rubric for the four missions revealed that all missions have very clear minimum and maximum bounds on possible points with the exception of mission 3. Given that mission 3 possessed the highest probability for maximum scoring, it was prioritized in the design trade study. Table 3.2.2 shows possible scoring outcomes assuming all missions are flown successfully.

Because the nature of mission 3 is unlike other missions that UCM has seen in past DBF competitions, initial sensitivity analysis took a naive approach by identifying relationships were that directly influenced the score for mission 3. These relationships were then studied separately without external influences in order to identify the constraints that would be most problematic for completing mission 3 with a high score. These more problematic constraints were then studied much closer.

Perhaps the most obvious constraint for mission 3 is the number of laps that the plane is capable of completing in 10 minutes. This constraint places a maximum bound on attack stores that the plane can drop. The number of laps that can be completed by cruising at different velocities can be visualized in figure 3.2.1 (a).

<b>Mission</b>	<b>Scoring Outcomes</b>
Mission 1	<ul style="list-style-type: none"> <li>• Results in one point for all teams (Eq. 3)</li> </ul>
Mission 2	<ul style="list-style-type: none"> <li>• Results in one to two points for all teams (Eq. 4)           <ul style="list-style-type: none"> <li>– The fastest team would only be ahead of the slowest team by one point</li> </ul> </li> </ul>
Mission 3	<ul style="list-style-type: none"> <li>• Allows the possibility of upsets in scores (Eq. 5)           <ul style="list-style-type: none"> <li>– All teams would get two points minimum for completion</li> <li>– Since all teams are required to have at least four attack stores, the minimum is potentially two points plus the four scoring laps (one for each of the four minimum required attack stores)</li> <li>– <u>The maximum score is not well defined</u></li> </ul> </li> </ul>
Ground Mission	<ul style="list-style-type: none"> <li>• Would result in a one or less score</li> </ul>

Table 3.2.2: Scoring Outcomes for Missions

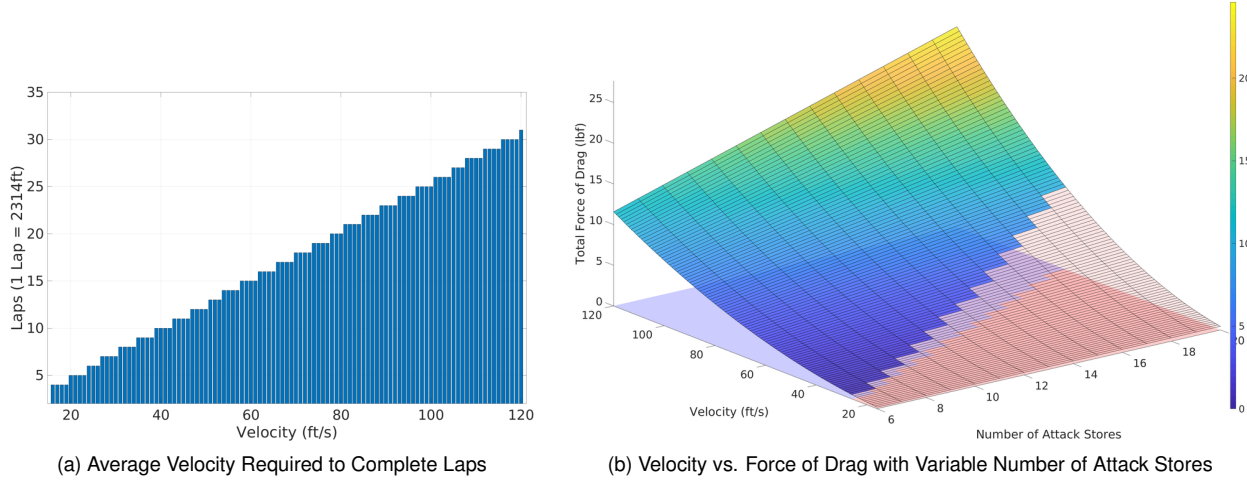


Figure 3.2.1: Analysis of Variables Related to Mission 3 Score

It is important to note that these velocities do not have to be maintained throughout the mission, but the average velocity must converge to these speeds in order to complete the corresponding number of laps. This fact brings attention to the next sub-figure.

A less obvious constraint for how many attack stores that can be successfully deployed for mission 3 is the capacity of the power source. The force of drag increases linearly for each additional attack store, and exponentially for faster velocities. These relationships are depicted in figure 3.2.1 (b). The red overlay on the force surface of figure 3.2.1 (b) is the projection of the minimum average velocity required to deploy the corresponding number of attack stores. Analyzing these relationships, the team found that the most efficient way to deploy attack stores for mission 3 is to start the mission by traveling slower than the required velocity and speeding up exponentially on each lap after dropping the attack stores.

By picking up speed exponentially after dropping each attack store, the team can maintain a constant drag force, which in turn relates to a constant level of battery usage that allows for better prediction of mission endurance and overall more efficient resource utilization. As long as the plane's average velocity during this mission converges to a greater than or equal velocity for the corresponding number of attack stores  $N_{stores}$ , all payloads will be successfully deployed under 10 minutes of flight, allowing for the highest score possible .

### 3.2.2 Ground Mission Analysis

Although the ground mission does not possess the capability of large upsets in scores like mission 3 does, the ground mission is still important because it creates leverage for the fastest team by enabling them to negatively impact opponent teams' scores. Focus on a fast ground mission time was not a high priority for optimization, however, while designing the attack store mechanism and radome, ease and speed of equipping these accessories were kept in mind. In addition, simple designs were assessed as having higher merit over complex designs for the following reasons:

- Simple designs are generally lighter weight designs.
- They are easier to manufacture.
- Will generally be easier and faster to secure. Prioritizing simpler designs directly influences the plane's ability for a fast ground mission.
- Reducing the amount of steps that have to be taken has a direct influence on ground mission operator performance, as cognitive load would be simplified.

## 3.3 Configuration Selection

### 3.3.1 Configurations Considered

An experimental high-level to low-level rapid prototyping selection process was used to select a preliminary aircraft configuration. The rapid prototyping allowed the team to quickly test the feasibility of various configurations in short ramp takeoff conditions. This approach essentially selected the best high level configuration that can be later refined by lower level configuration optimization to meet mission requirements. Three configurations were selected as candidates (shown in figure 3.3.1) and then narrowed down to one by imposing a selection criterion that takes into account the four mission requirements for the 2019 DBF competition year.

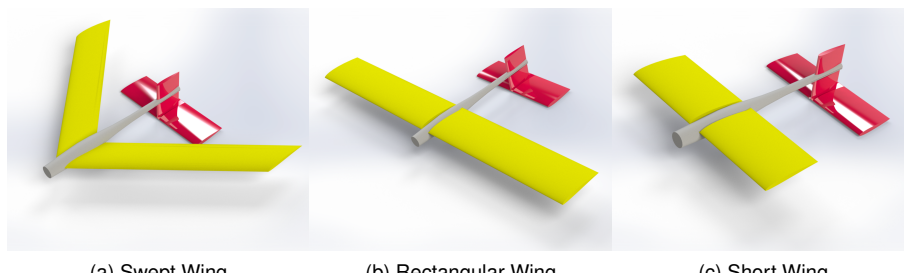


Figure 3.3.1: Considered Wing Configurations

The first configuration built by the team and tested for short take off characteristics was the swept wing cargo configuration. The methodology behind the selection of the swept wing cargo prototype was (1) to carry as many attack stores as possible, and (2) achieve higher stable mission flight speeds since the plane utilized a swept wing. Key design features of this configuration include:

- The swept wing increased lift and roll of the aircraft and produced less induced drag, which acted as a “dihedral” in terms of pulling the aircraft back into place, an attractive feature for increasing flight stability at higher speeds when attack stores are released
- The swept wing provided yaw stability, due to increased length of the wing
- Placing the control surfaces at the wingtips, the sweep decreased the lever arm of the control surface, causing smaller moments to be produced by them
- Higher degree of sweeps reduces the need of washouts, due to the natural static stability of swept wing designs, reducing plane weight
- Stall velocities and unwanted characteristics are effectively lowered by the sweep, making landings easier

The second configuration considered was a conventional high rectangular wing design with an angle of attack of 5 degrees and higher AR. The methodology behind the consideration of the high flat wing conventional design was (1) to determine the feasibility of an aircraft that performed missions at slower speeds, but provided more lift at takeoff ramp conditions, and (2) having a higher aspect ratio (AR) wing that naturally induces latitudinal stability during the attack store launch process. Some of the key highlights of this configuration:

- A rectangular wing has strong wing tip vortices reducing the effective angle of attack at the tips, delaying a tip stall leading to desirable stall characteristics vs. other configurations
- The easiest to manufacture and repair in the advent of a failed launch due to ramp takeoff conditions
- The higher AR makes this configuration more resilient to changes in latitudinal CG when attack stores are dropped, most prominently when attack stores are mounted as close to the fuselage as possible
- A conventional rectangular wing is easiest to fabricate with strong structural characteristics, allowing the team to further increase the AR if desired while keeping the chord length to a minimum for packaging purposes

The 3rd configuration was a short wing aircraft that implemented long chord lengths for short take off conditions. The methodology behind this consideration for this short wing configuration was (1) high speed mission capability, and (2) attractive low structural weight that will allow more attack store payload capability. Some of the key highlights of this configuration:

- The value of the section drag coefficient is an inverse logarithmic function of the characteristic length of the surface ( $C_d \propto 1 / (Chord)^{0.129}$ ), indicating that a shorter wing span allows for high flight speeds with the least amount of parasitic drag
- A short wingspan configuration results in lower aircraft weight due to structural simplifications, allowing a higher flight payload capability

- Quick roll rates due to the lower moment of inertia associated with shorter wingspans, allowing more maneuverability to quickly execute missions in high payload situations

### 3.3.2 Configurations Selection Process

The configuration selection process uses a set of criterion devised from mission requirements to generate Figures of Merit (FoM) presented in table 3.3.1. The FoM take into account the most important factors that impact aircraft mission performance and construction, qualitatively derived in context with the design and mission requirements for the 2019 DBF Rule set. Each FoM was assigned an importance factor of 0-5, from least to most important to the mission requirements. All configurations are comprehensively weighed against the FoM, with the most points accumulated by one configuration being the selected configuration for the 2019 DBF contest year. The methodology behind the weighing process of the FoM is described in table 3.3.1.

Considerations	Merit Factor
Weight	5
Ramp Takeoff Suitability	5
Flight Speed	4
Packaging Complexity	3
Flight Stability	3
Repairability	3
Manufacturing Complexity	2

Table 3.3.1: Figures of Merit

- **Weight** is defined as the aircraft's ability to maintain the lowest total weight after construction, including all subsystems, without payload. Due to the 10 ft takeoff ramp constraints, the team acknowledged that weight is a critical factor that directly affected the aircraft's ability to score highly, by limiting its capability to carry more attack stores and take off within 10 ft. Weight received the highest FoM weight, 5.
- **Ramp Takeoff Suitability** is defined as the configuration's inherent design with dealing in short take off situations. This factor takes into account the amount of lift that an aircraft can generate in 10 ft at a given speed, wing geometry, and wing lift characteristics. The Ramp Takeoff Suitability factor also takes into account current lift improvement techniques such as vortex generators, leading edge slats, and wing tip geometry for vortex generation control. *Missions 1-3 cannot take place unless the aircraft is successfully launched from the ramp, hence the Ramp Takeoff Suitability weight is given a value of 5.*
- **Flight Speed** is defined as the maximum flight speed the aircraft is able to sustain due to it's wing geometry and characteristics. *Given that flight missions 2-3 are time dependent, with mission 3 providing the opportunity to score the highest of all missions, the Flight Speed weight was given a value of 4.*
- **Packaging Complexity** factor is defined as the complexity required to make a configuration reach all flight and ground packaging requirements, assigned a weight value of 3.

- **Flight Stability** is defined as the an aircraft's ability to fly in a stable manner and remain stable when CG changes occur once attack payloads are released during mission execution. Stability is a subjective value relative to the skill set of the pilot, hence it was assigned a weight value of 3.
- **Repairability** is defined as the simplicity of repairing a configuration if any failures occur during mission attempts. If failures occur and repairability is too difficult, this can lead to the team having to forfeit future mission attempts. The weight was assigned a value of 3.
- **Manufacturing Complexity** is defined as the ease of manufacturing, including all sub-assemblies required to satisfy the packaging requirements (stowed configuration) of the competition. Manufacturing complexities do not directly affect mission performance, however it has great affects on the team's ability to manufacture and test various prototypes of a configuration in a timely manner. The Manufacturing Complexity weight was assigned a value of 2.

<b>Figures of Merit (FoM)</b>	Score Weight	Swept Cargo Plane	<b>Con. High Rect. Wing</b>	Short Wing
Weight	5	3	4	5
Ramp Takeoff Suitability	5	3	5	3
Flight Speed	4	4	3	5
Packaging Complexity	3	3	5	4
Flight Stability	3	4	4	3
Repairability	3	3	4	5
Manufacturing Complexity	2	3	4	5
	Total Score	82	<b>101</b>	97

Table 3.3.2: Aircraft Configuration Selection

As indicated in the Aircraft Configuration Selection table 3.3.2, the High Wing Conventional design was the most ideal for the 2019 DBF requirements, despite being the slowest of the three configurations presented. The short wing received a Takeoff Suitability score of 3. This was because the short wing would be the most impacted by the attack stores' weight and drag. The speed advantages of the short wing are only effective at very high speeds, not enough to offset the capabilities of higher AR geometries. Drag is dependent on the wing AR and lift is proportional to the wing area, but the lift to drag ratio is proportional to the wing AR. A higher AR is preferred due to minimized energy loss. Having the advantage in Ramp Takeoff over the Short Wing configuration and the advantage of lower weight over the Swept Cargo Plane configuration is more critical to the *reliability* of mission performance than being the fastest configuration of the three. Despite achieving lower flight speeds, the High Wing Conventional design guarantees short ramp takeoff and higher payload capability.

### 3.4 Configuration Optimization For Mission Requirements

After selecting the highest scoring configuration, the team proceeded to refine the conceptual design low level configurations, to meet payload, aircraft packaging, and tail design requirements.

### 3.4.1 Wing Configuration

A higher AR rectangular mid-wing was selected for the wing configuration due to its predictable stall behavior, ease of manufacturing, and greater usable surface area that is unaffected by the attack stores during takeoff. The selected configuration was further optimized in the following critical ways to improve mission performance:

- The 5 degree AoA was reduced to a one degree AoA, requiring the aircraft to fly at faster speeds to maintain altitude, effectively increasing the speed of the aircraft during missions
- The reduced takeoff ability was completely offset by (1) employing elevator and aileron radio controlled mixing to create "flaperons", the equivalent of flaps, and (2) using vortex manipulation techniques such as Horner Wing Tips to increase the effective wingspan of the wings during takeoff
- The wings employ a rectangular geometry, an ideal geometry for predictable stall behavior given the lift distribution produced, pictured in figure 3.3.1, allowing the wing root to stall before the tip
- The wings were also adapted to a mid-wing configuration, to provide more roll control in high payload configurations

### 3.4.2 Wing Packaging Approach

The team considered many packaging configurations to meet the requirement of having the aircraft being capable of fitting inside a space of 3 ft wide and 2 ft high in the stowed condition. Three of the most desirable configurations were considered. Similarly to the high level configurations selection, a FOM was created with respect to mission requirements and constraints imposed.

- **Ball Joint Wing:** The folding wing was considered due to it's common place amongst full size aircraft and was inspected to see the viability of it's use for the 2019 DBF missions. A linearly upward folding wing was not desired due to the 3 ft wide and 2 ft high stowed condition, thus it was modified to fold in 2 degrees of freedom, upward and backward. The design utilized a ball joint mechanism that allowed the wings to lift up, rotate 90 degrees, and pivot backwards. The 2 DoF folding wing was attractive for structural reasons, it allowed the main spar to be continuous. However, designing this configuration to be capable of self transitioning and locking into flight mode leads to over complications within the wing sub-architecture. [4]
- **Hinged Wing:** The wing hinge historically has been one of the most popular ways to rotate the wing back into a stowed configuration. Unlike the Ball Joint Wing, the wing hinge requires only one degree of freedom, simplifying the actuation process. However, this actuation still has to take place within the wing, adding more structural complexity within the wings that is undesirable.
- **Pivot Wing:** The pivot wing configuration utilizes a central structure that the wings mount to. This central structure absorbs all loading from the wing and effectively acts as a central spar joining the two wings. The main advantage of the pivoting wing is that the actuation mechanisms do not have to be built within the wing, simplifying the manufacturing process of the wing and allowing it to be more repairable in the event of a mishap. The actuation can take place within the within the central structure, or the fuselage. Another

advantage of this mechanism is that it only needs a one degree of freedom actuation, further simplifying the automation process.

<b>Figures of Merit (FoM)</b>	Score Weight	Ball Joint Wing	Hinged Wing	<b>Pivot Wing</b>
Weight	5	2	3	4
Strength	4	4	4	3
Simplicity	3	2	3	4
	Total	32	37	<b>44</b>

Table 3.4.1: Wing Packaging Options & Their Corresponding Figures of Merit

Based on the results in table 3.4.1, the best configuration to meet the packaging requirements in the most efficient way is the Pivot Wing configuration, offering the highest balance of strength, induced weight, and simplicity to manufacture.

### 3.4.3 Tail Configuration

The addition of a radome on top of the aircraft introduced flow complexities that had to be accounted for when choosing tail configuration. Four tail configurations were considered, a conventional tail, off-set conventional tail, T-tail, and V-Tail. All options were evaluated for the viability of their use in meeting mission requirements and weighed using a Figure of Merits.

- **Conventional Tail:** Usually provides adequate stability, control, reliability, and are easy to manufacture. The issue with conventional tails is that they may be present within the downward flow stream in the wing, affecting the tail's ability to provide control and stability.
- **T-tail:** Is superior for control, and having "clean" air, away from the downstream of the wing. However, they are slightly more sensitive structurally, reduce torsional eigenfrequency due to the long lever-arm, and are prone to deep stalls. For mission 2 requirements, the T-Tail may impose issues since the air flow to the tail will be disturbed due to interference from the radome.
- **V-Tail:** The V-tail was considered for its attractive geometry setup that allows it to perform better in conditions where upstream air flow may be disrupted by the wing, fuselage, and radome. However, it is harder to manufacture and has a few undesirable effects such as "fish tailing" and rolling characteristics when strong side wings are present.
- **Offset Conventional Tail:** The offset conventional tail (figure 3.4.1(c)) builds upon all the benefits of a normal conventional tail with the additional of a slight offset that removes the horizontal stabilizer away from unwanted upstream effects caused by the wing, fuselage, and radome. This allows the team to use a simple linear fuselage-tail boom connection and maintain adequate elevator control.

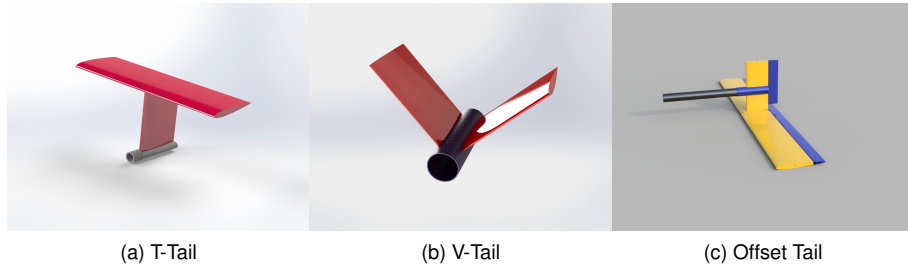


Figure 3.4.1: Considered Tail Configurations

<b>Figure of Merits (FoM)</b>	Score Weight	Conventional	T	V	<b>Offset Conventional</b>
Weight	5	5	5	3	5
Manufacturability	4	5	4	3	5
Stability	4	4	3	4	4
Control	3	3	4	4	4
Total		70	65	55	<b>73</b>

Table 3.4.2: Tail Configuration Options & Their Corresponding Figures of Merit

Based on the results from table 3.4.2, the offset conventional tail provided the best results based on the graded values derived for the mission requirements. It is easy to manufacture, and remains out of the undesirable upstream flow conditions, providing adequate stability and control as a result.

#### 3.4.4 Attack Store Configuration

Choosing the configuration for the attack stores required the consideration of (1) drag, (2) complexity of the mechanism that a configuration would give rise to, (3) stability effects on the aircraft. Drag affects the maximum flight speed that the aircraft is capable of sustaining, and the complexity of the mechanism affects the takeoff weight of the aircraft. Mission 3 provides the highest scoring opportunity, thus the attack store configuration is optimized for mission 3, via the prioritization of the minimization of weight induced by the complexity of the mechanism configuration. Two configurations were considered and then weighed against a FoM devised with respect to critical mission scoring needs.

- **Chord Bias Configuration:** The span bias configuration starts off by mounting the first 4 attack stores along the span of the wing and any additional stores are mounted behind each other. This setup reduces drag contributed from additional attack stores, however it introduces manufacturing and actuation complexities that lead to more weight, affecting the number of attack stores that the aircraft can launch with. Additionally, the stability of the aircraft is affected in the longitudinal and latitudinal directions when a launch sequence is made, further introducing complexities due to two way CG shifts.
- **Span Bias Configuration:** The span bias configuration (figure 3.4.2 (b)) starts off by mounting the first 3 attack stores along the span of the wing and any additional stores are mounted linearly along the span of the wing as well. This setup creates additional drag induced by the each attack store, an undesirable effect

directly affecting the maximum sustainable speed of the aircraft. Stability changes however only affect the CG in the latitudinal direction. A linear setup allows the launch mechanism to be straightforward and very lightweight.

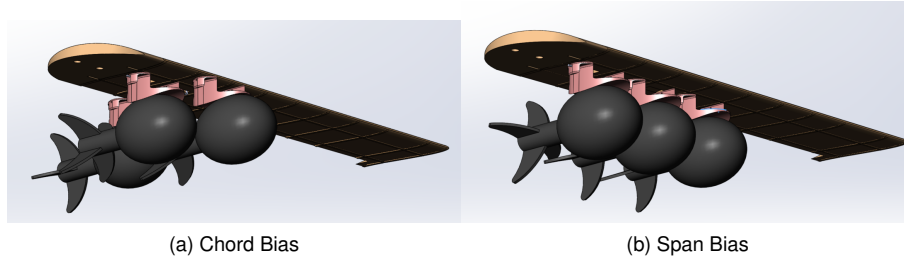


Figure 3.4.2: Considered Store Configurations

<b>Figures of Merit (FoM)</b>	Score Weight	Chord Bias	<b>Span Bias</b>
Weight	5	3	5
Stability	4	3	4
Flight Speed	3	5	3
	Total	42	<b>50</b>

Table 3.4.3: Attack Store Configuration Options & Their Corresponding Figures of Merit

From the FoM presented in table 3.4.3, the span bias configuration was the most optimal based on the attack store configuration selection methodology. Important weight savings are crucial due to the constraint ramp takeoff conditions, directly affecting the amount of attack store drops that can be attempted.

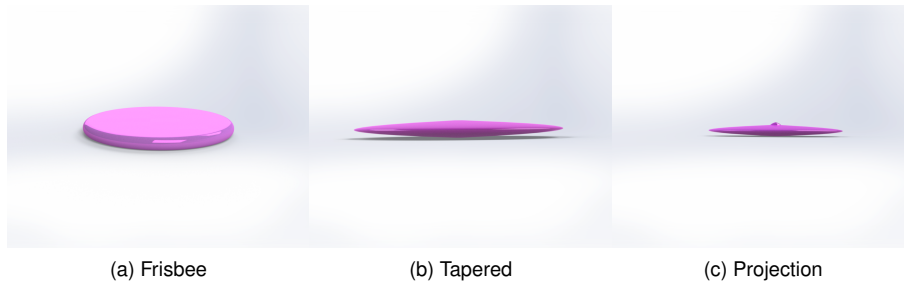
### 3.4.5 Radome Configuration

The introduction of the rotating radome introduces airflow complexities that directly impact the flight characteristics of the aircraft and need be accounted for in the overall design. The additional drag alters the maximum flight speed and airflow disturbances can interfere with other aircraft components. Because the radome must rotate in flight it was determined that the overall shape should be symmetrical and circular so that no one side caused more drag. Three shapes that met both our constraints and the ones outlined in the competition rules were analyzed, a Frisbee shaped radome, a tapered radome, and a projection radome. Each was analyzed and evaluated to determine its practicality in meeting mission requirements and was weighed using a Figure of Merit.

- **Frisbee Radome:** Figure 3.4.3 (a) is a constant 1 inch thick disk with a diameter of 12 inches and has curved edges to direct airflow above and below the feature. This model is sufficiently stable and simplistic in nature for easy manufacturing. However, it produced the highest drag of the three configurations with a large separation bubble on the trailing edge creating vortices that could interfere with other components of the aircraft such as the tail.
- **Tapered Radome:** Figure 3.4.3 (b) consists of a disk with a taper from the 1 inch thick center to thin curved edges. This shape is highly stable and created the least drag of the configurations due to a smaller

separation bubble on the trailing edge. The radome must be fabricated such that it is exactly symmetrical on the top and bottom so that no lift will be produced. The main drawback to this design is that no hardware can be mounted inside the radome without reducing the thickness from the required 1 inch minimum at the center.

- **Projection Radome:** Figure 3.4.3 (c) is similar in shape to the tapered radome but with a quarter-inch protrusion on top at the center, it also has similar characteristics to the tapered radome but with slightly extra drag due to the protrusion on top. It was considered due to the overall thickness allowing for the radome to meet the one-inch minimum thickness requirement while having the option to mount hardware for rotating the radome, like gears, inside the radome itself.



(a) Frisbee

(b) Tapered

(c) Projection

Figure 3.4.3: Considered Radome Configurations

<b>Figures of Merit (FoM)</b>	Score Weight	Frisbee	Tapered	Projection
Manufacturing Complexity	3	3	2	1
Stability	4	2	4	3
Drag	5	2	5	4
	Total	27	<b>47</b>	35

Table 3.4.4: Radome Configuration Options & Their Corresponding Tables of Merit

The results indicated by table 3.4.4 show that the ideal configuration is the tapered radome. It is crucial that the drag from this feature be minimized while still meeting the constraints stated in the rules.

### 3.5 Final Conceptual Design

A mid-wing wing offset conventional tail with a pivoting wing configuration (shown in figure 3.5.1) has been chosen as the most optimal design for the constraints and requirements presented by the 2019 Design/Build/Fly competition.



Figure 3.5.1: Final Conceptual Design

## 4 Preliminary Design

The objective of the preliminary design was to further optimize the aircraft characteristics and properties to better meet mission requirements. The primary goals were to (1) maximize the amount of attack store payload that the aircraft is able to carry for mission 3, (2) maximize the speed of the aircraft is able to sustain for mission 2, and (3) maximize the payload loading/unloading techniques. All goals are accomplished with respect to the requirements presented by the 2019 Design/Build/Fly ruleset.

### 4.1 Design Methodology

Thunder\_Cats used a design methodology that leverages the team's custom software, DTS\_Cat, to generate simulation models of the aircraft based on inputs from design trade studies. The methodology consisted of (1) using DTS\_Cat V3 to fine tune the *approach* for the aircraft design trade studies and (2) *designing* the aircraft using an iterative, comprehensive, and multidisciplinary analysis to ensure all mission requirements are met with an emphasis on mission 3 performance.

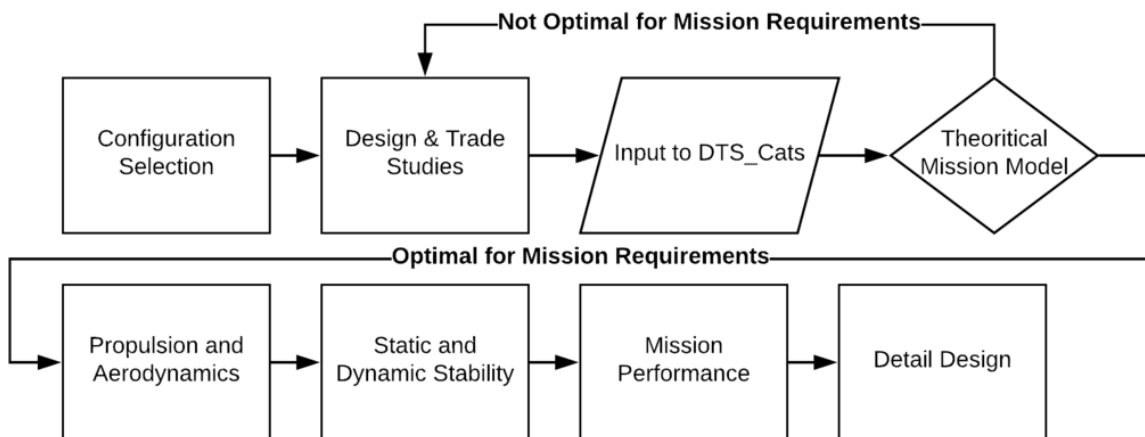


Figure 4.1.1: UML Diagram of the Design Methodology

Figure 4.1.1 demonstrates that DTS\_Cat was used as a tool that fine tuned approaches taken by the team in the design trade process, allowing the team to quickly verify if their theoretical data meets optimal mission requirements. When the theoretical data that the team generated in the design trade study process met performance requirements, the team progressed on to downstream processes that generated an optimal preliminary design, adequately meeting all of the team's performance requirements with respect to the missions.

## 4.2 DTS\_Cat

In order to run quick simulations with different variables in place, the simulation engineers developed DTS\_Cat, a MATLAB based tool that generated graphs and output other important variables useful in fine-tuning parameters for the design team to fulfill (Here, DTS is an acronym for Design Trade Sensitivity).<sup>[1]</sup> This tool was developed in a top-down manner, integrating the fundamental equations of motion and equations of lift to generate plots that demonstrated the viability of different configurations relative to constraints (1), (2) and (3) presented in the Executive Summary, section 1 of the report. As further needs developed and the geometry of the plane was constrained based on results from the tool, DTS\_Cat was further refined to meet the needs of the team.

Due to missions 1-3 requiring taking off on a 10 foot ramp with a 5° incline, the team placed priority on ensuring the capability of the plane and perfecting the necessary variables required for successful takeoff. These calculations laid the foundation for the plane design and architecture by establishing limits of variables that guarantee flight from the ramp in conditions comparable to historical data on Arizona's April climate. Appropriate safety factors were placed on these variables to guarantee flight in various unforeseen conditions.

**DTS\_Cat V1:** The initial basic variables in DTS\_Cat V1 were lift  $F_l$ , plane weight  $W_{plane}$  and thrust  $F_t$ . These were utilized to estimate a reasonable weight for the plane to be able to take off on the provided 10 foot inclined ramp. The lift and thrust figures were estimated based via the limitation of NiMH battery pack outputs and masses they contribute to the overall weight of the plane.

The results showed that empty plane weight had to be extremely light, lighter than previous DBF builds from UCM, and must be capable of creating lift that overcomes weight at a very low speed. Thrust will also need to surpass the amount of force required for the plane to reach this speed within 10 ft in addition to the trivial amount of gravity counteracting thrust caused by the 5° incline. Thus drastic optimization had to take place to reduce minimum flight speed,  $Min_{speed}$ , to the lowest value possible.

**DTS\_Cat V2:** To achieve the lowest  $Min_{speed}$  required, further development on DTS\_Cat was needed. Lift, plane weight and thrust were changed from input variables to expressions comprised of much more detailed input parameters, allowing the simulation team to fine tune different flight geometries of the plane to determine viability of different inputs. This allowed the team to generate realistic numbers based on realistic input of plausible design parameters acquired from trade studies. The high level fundamental equations used are listed in equations 7-10.

$$W_{total} = W_{plane} + [W_{store} \cdot N_{stores}] + [W_{batt} \cdot N_{batts}] \quad (7)$$

Eq. 7 demonstrates the weight of the whole plane in pounds including attack stores and batteries.

$$F_l = \frac{1}{2} \rho(v^2) L_{ws} L_{wc} Cl \quad (8)$$

Eq. 8 represents the lift of the plane in pounds based on wing properties and dimensions at different speeds. This equation runs iterative so that the team can compare the weight and lift of the plane to establish the minimum speed required for flight.

$$\text{Min}_{\text{speed}} = v \text{ where } F_l = W_{\text{total}} \quad (9)$$

The minimum speed is represented in Eq. 9, defined as the speed where the force of lift generated by the plane is equal to the weight of the plane, thus flight starts to become feasible at this speed.

$$F_t = \left( \frac{W_{\text{total}}}{32.2} \right) \left( 32.2 \sin(5^\circ) + \frac{\text{Min}_{\text{speed}}^2}{20} \right) + \text{Drag}_{\text{wing}} + \text{Drag}_{\text{fuselage}} + \text{Drag}_{\text{tail}} + \text{Drag}_{\text{ATK}} \quad (10a)$$

$\text{Drag}_{\text{wing}}$  is defined as:

$$\text{Drag}_{\text{wing}} = \frac{1}{2} C_d_{\text{wing}} \cdot \rho \cdot L_{ws} \cdot \text{Height}_{\text{wing}} \cdot \text{Min}_{\text{speed}}^2 \quad (10b)$$

$\text{Drag}_{\text{fuselage}}$  is defined as:

$$\text{Drag}_{\text{fuselage}} = \frac{1}{2} C_d_{\text{fuselage}} \cdot \rho \cdot \text{CSA}_{\text{fuselage}} \cdot \text{Min}_{\text{speed}}^2 \quad (10c)$$

$\text{Drag}_{\text{tail}}$  is defined as:

$$\text{Drag}_{\text{tail}} = \frac{1}{2} C_d_{\text{TVS}} \cdot \rho \cdot L_{\text{TVS}} \cdot \text{Height}_{\text{TVS}} \cdot \text{Min}_{\text{speed}}^2 + \frac{1}{2} C_d_{\text{THS}} \cdot \rho \cdot L_{\text{THS}} \cdot \text{Height}_{\text{THS}} \cdot \text{Min}_{\text{speed}}^2 \quad (10d)$$

$\text{Drag}_{\text{atkstores}}$  is defined as:

$$\text{Drag}_{\text{ATK}} = \frac{1}{2} C_d_{\text{attackstore}} \cdot \rho \cdot N_{\text{stores}} \cdot A_{\text{attackstore}} \cdot \text{Min}_{\text{speed}}^2 \quad (10e)$$

Eq.s 10 a-d are the equations used by DTS\_Cat V2 for the force required to accelerate the plane from 0 ft/s to the minimum flight speed defined from Eq. 9 on the 5° incline. Although negligible at low speeds, as a safety factor, these equations account for drag of the fuselage, wing, vertical and horizontal stabilizers and stores. The approximate coefficients of drag for our attack stores were acquired from SOLIDWORKS Flow Simulations that the team ran on comparable attack stores.

With the help of DTS\_Cat V2, the team was able to make the first 10 foot ramp flight attempt a success. The prototype plane that the team used for first flight matched the parameters tested in DTS\_Cat V2 and successful takeoff on the ramp confirmed the accuracy of the simulations team's code.

**DTS\_Cat V3:** Version 3 of DTS\_Cat had incremental modification that included a verification component that ensured the batteries would provide enough energy to complete the number of laps required to drop each of the chosen number of attack stores for mission 3. In addition, the verification check was expanded to ensure that the batteries, motors and propeller chosen could achieve the force required for takeoff without surpassing battery

drain limits.

$$P_{req} = 1.415 \cdot v \cdot (Drag_{wing} + Drag_{fuselage} + Drag_{tail} + Drag_{attackstores}) \quad (11a)$$

$Drag_{wing}$  is defined as:

$$Drag_{wing} = \frac{1}{2} Cd_{wing} \cdot \rho \cdot L_{ws} \cdot Height_{wing} \cdot v^2 \quad (11b)$$

$Drag_{fuselage}$  is defined as:

$$Drag_{fuselage} = \frac{1}{2} Cd_{fuselage} \cdot \rho \cdot CSA_{fuselage} \cdot v^2 \quad (11c)$$

$Drag_{tail}$  is defined as:

$$Drag_{tail} = \frac{1}{2} Cd_{TVS} \cdot \rho \cdot L_{TVS} \cdot Height_{TVS} \cdot v^2 + \frac{1}{2} Cd_{THS} \cdot \rho \cdot L_{THS} \cdot Height_{THS} \cdot v^2 \quad (11d)$$

$Drag_{attackstores}$  is defined as:

$$Drag_{attackstores} = \frac{1}{2} Cd_{attackstore} \cdot \rho \cdot N_{stores} \cdot A_{attackstore} \cdot v^2 \quad (11e)$$

Eqs 11 a-e were used by DTS\_Cat V3 to estimate the power required of the battery to maintain velocity  $v$  at any given time. The team included a safety factor of 1.415 to the actual power required in order to account for any inefficiencies of the electrical propulsion system due to heat, unaccounted for propeller inefficiency, and other unaccounted for variations.

Input Variable	Parameter to Model	Output Variable	Flight Characteristic
$N_{stores}$	Number of Stores to Test	$Min_{speed}$	Minimum Flight Speed Achievable
$N_{batts}$	Number of Batteries	$P_{req}$	Power Req. to Cruise at $v$
$W_{plane}$	Weight of Empty Plane	$F_t$	Force Req. for Takeoff (W/ Ramp)
$W_{batt}$	Weight of a single Battery	$W_{total}$	Total Plane Weight When Equipped
$Cl$	Coefficient of Lift	$N_{laps}$	Number of Laps Capable (W/Stores)
$\rho$	Density of Air	$CHK_{takeoff}$	Boolean Check: Takeoff Capable?
$Cd_{wing}$	Coefficient of Drag (Wing)	$CHK_{laps}$	Boolean Check: $N_{store}$ Laps Capable?
$P_{batt}$	Power of One Battery		
$Height_{wing}$	Wing/Airfoil Thickness		
$L_{ws}$	Length of Wings		
$L_{wc}$	Length of the Wing Chord		

Table 4.2.1: Some Input and Output Parameters of DTS\_Cat MATLAB Software

<b>Output Variable</b>	<b>DTS_Cat's Influence on Design Architecture</b>
$Min_{speed}$	Lower speeds indicated to the team that the lift-to-weight ratio for the emulated model was a good design decision
$P_{req}$	Helped the team decide on the minimum capacity required of battery pack(s) to sustain longer flights with more attack stores
$F_t$	Lower force required for takeoff indicated easier takeoff and the capability of carrying more attack stores
$W_{total}$	Aided the team in choosing the lightest configuration of batteries still capable of takeoff and completing the necessary laps
$N_{laps}$	This only needed to exceed the number of attack stores being carried, so if this number was too high, the team reduced the battery capacity for weight reduction
$CHK_{takeoff}$	This check saved the team time with rapid prototyping by immediately indicating major design flaw in the emulated model
$CHK_{laps}$	This check saved the team time with rapid prototyping by immediately indicating major design flaw in the emulated model

Table 4.2.2: How calculations from DTS\_Cat influenced design architecture decisions

Completion of DTS\_Cat V3 meant the team was able to quickly input and receive the data listed in table 4.2.1. The tool was extremely valuable in rapid prototyping and saved the team a lot of time by filtering design ideas that could and could not work based on the results. Later the software became useful in aiding the team to fine-tune parameters for mission 3, in an attempt to maximize the team's total score and ultimately helped the team come to final design decisions. Some influences of the software are outlined in table 4.2.2

## 4.3 Design Trade Studies

### 4.3.1 Wing Geometry

Wing span was one of the main constraints in the design, directly affecting the aircraft's (1) ability to reliably takeoff from the takeoff ramp, (2) mission flight speed, and (3) weight of the aircraft. Wing geometry trade studies had to factor in (1), (2), and (3), striking a balance between the three constraints for optimal mission performance. The wing had no span wise constraint for the 2019 DBF ruleset other than the 4 ft minimum span. This gave the team the freedom to choose a wing span that allowed the highest amount of attack store payload as possible. However, increasing the wing span had the following two key limiting effects:

- **Fuselage Tipping:** Increasing the wing span meant that more mass would be deflected towards the rear of the aircraft in the stowed configuration. This deflection of mass causes a CG transition to occur, shifting the CG to the rear and increasing chances of the aircraft tipping. With the 2 ft landing gear limit imposed on the aircraft, a model had to be generated that calculates how long the span of the wing could be, before tail tipping effects are induced in the stowed configuration

- **Weight:** A long wingspan means that weight begins to increase exponentially due to the required structural reinforcement. Furthermore, fluttering becomes a problem as well.

Using the knowledge that longer wing spans cause undesirable shifts in the longitudinal CG that directly affected the aircraft's ability to remain stationary during the stowed configuration, the team used DTS\_Cat to model the shift in CG that different wing spans induce. Based on the results from figure 4.3.1, a wing span of 80" was the most efficient geometry, changing the CG within the allowable range of 8 in rearward. This optimization increased the lifting area of the wing by 33% while only affecting the total weight of the aircraft by 3.2 ounces. The change from the original geometry, coupled with the implementation of vortex generators and advanced winglets, allowed the team to carry an addition of 4 attack stores. The wing AR is 10.465.

### 4.3.2 Propulsion System Sizing

The propulsion system was designed to produce enough power for takeoff during all flight missions, while still being as light and efficient as possible. The heaviest component of the propulsion system is the NiMH battery packs. Thus optimizing energy storage for the duration of the mission while retaining take off capability is crucial. The most energy demanding mission is mission 3, where the full attack store payload must be flown, and the number of laps must match the number of To achieve a maximum power output and flight time, a 22V battery pack attack stores. This is a very demanding task and the battery packs must have a large amount of energy.

$$Power = Voltage \times Current \quad (12)$$

$$Energy = Power \times Time \quad (13)$$

with 1500mAh was proposed. The energy estimation of the battery pack was 33Wh, allowing approximately 130W power consumption for 15 minutes.

$$Energy = 22V \times 1.5Ah \quad (14)$$

A mathematical model of the plane was used to determine the approximate power required for the plane to fly at various air speeds. Minimum flight speeds for 10 attack stores comes out to be 25ft/s, giving the team the advantage of a large operating range for air speed. The conclusion was the required power will range from 80-150 watts at the minimum air speed, showing that the initial battery selection was accurate for the plane. However, due to inefficiencies and wind speeds, the battery may need to be 66Wh in the current configuration, which still will allow a 10ft take off at full payload.

Motor selection was then found using the same software to show to the minimum required thrust for takeoff on

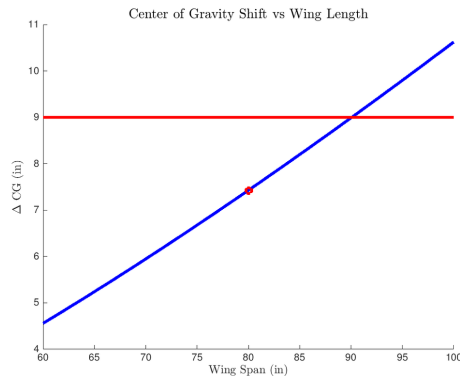


Figure 4.3.1: Change in CG vs Wing Length

a 10 ft runway at 5 degrees above horizon. With full payload, the thrust needed for take off came to about 4.5-5 lbf, which was calculated with the inefficiencies of the propeller and the motor. The motor selected was a Cobra 980Kv, which is capable of producing 5.2 lbf of thrust with a 9X4.5 APC propeller (shown in table 4.3.1).

<b>Motor</b>	<b>Battery Pack</b>	<b>Propeller</b>
Cobra C-3520 Brushless	18 × Elite 1500mAH (22.8V)	APC 9 × 4.5

Table 4.3.1: Motor, Battery Pack and Propeller specs

#### 4.4 Mission Model

The mission model presented is the final and most optimal mission model that team Thunder\_Cats modelled using DTS\_Cat. In this section, the ideal model that this aircraft has been designed for is presented along with uncertainties.

- **Takeoff:** Utilizing vortex generators and flaperons to effectively increase  $C_L$  to a value of 2.6, the aircraft will be able to take off at 22 ft/s with 12 attack stores. Terminal velocity within 10 ft of the ramp at an incline of 5 degrees was expected to be 24 ft/s. This approximation does not factor in any head wind that effectively increases airspeed over the wings, and thus lift.
- **Climb:** Kirin was designed to climb to an altitude of 100 ft above the 2650 ft (approximated) ground level of Tucson, Arizona, at a rate of 16 ft/s. The rate of climb was approximated using the difference between the thrust force the propulsion system was capable of producing and drag force imposed on the aircraft.
- **Cruise:** The aircraft was designed to cruise at 80 ft/s. The cruise speed was modelled by finding the most optimal throttle output based on the capabilities of the propulsion system, battery life consumption rate, and when aircraft forces are in aerodynamic equilibrium. Furthermore in mission 3 the cruise speed increases as attack stores are dropped each lap, maintaining the balance between drag and thrust forces, and keeping the propulsion system operating within the most efficient range.
- **Turn:** Turn rate was modelled to be at 60 ft/s within a radius of 32 ft, including an altitude drop of about 20 ft. Turns are executed at high throttle levels to minimize altitude loss and possibility of stall.

Where assumptions made for the model simulation are:

- **Wind:** The average wind speed from the last Design/Build/Fly competition was 13.5 MPH. The takeoff simulation of the model did not factor in this headwind to allow a higher factor of safety for take off.
- **Battery Performance:** Assumes that an ESC governor is used to maintain RPM and thrust output as voltage sags, replicating an ideal battery.
- **Propeller Performance:** Propeller performance is assumed to have an efficiency of 70% during cruise flight while, and 80% during takeoff, based on manufacturer propeller data charts.

Model Uncertainties uncertainties include:

- The model assumes that the governor function of the ESC is used, and thus uses an ideal battery for

internal simulation. This may lead to inaccuracies since this does not take into account the effect of when the governor reserves become ineffective.

- The model does not account for varying headwind for takeoff conditions or headwinds exceeding 13.5 MPH for cruising flight conditions. A strong headwind in takeoff conditions would allow the team to carry more attack stores, however a strong headwind in cruise conditions would overstrain the propulsion system resulting in early termination of flight.
- Pilot error is unaccounted for.
- Atmospheric stability in the form of the local atmospheric boundary conditions, such as boundary layer height and local airspeed fluctuations within a certain region, are not accounted for in the model.

## 4.5 Aerodynamics

### 4.5.1 Airfoil Selection

The airfoil selection was important for the aircraft design for efficiency and ability to have an attack store dropping mechanism inside of the wing. The largest necessity for the airfoil was a high coefficient of lift within the air conditions in Arizona. The SA7036 fit this role, and has sufficient thickness for the store dropping mechanism. In addition to sufficient thickness, this airfoil has minimal drag, and at the maximum coefficient of lift of 1.3, the maximum coefficient of drag is 0.035, which is crucial for mission performance.

The other best candidate airfoil compared was the NACA 2408. Shown in figure 4.5.1 is the comparison of the airfoils in the mid range Reynolds number the plane will experience in flight.

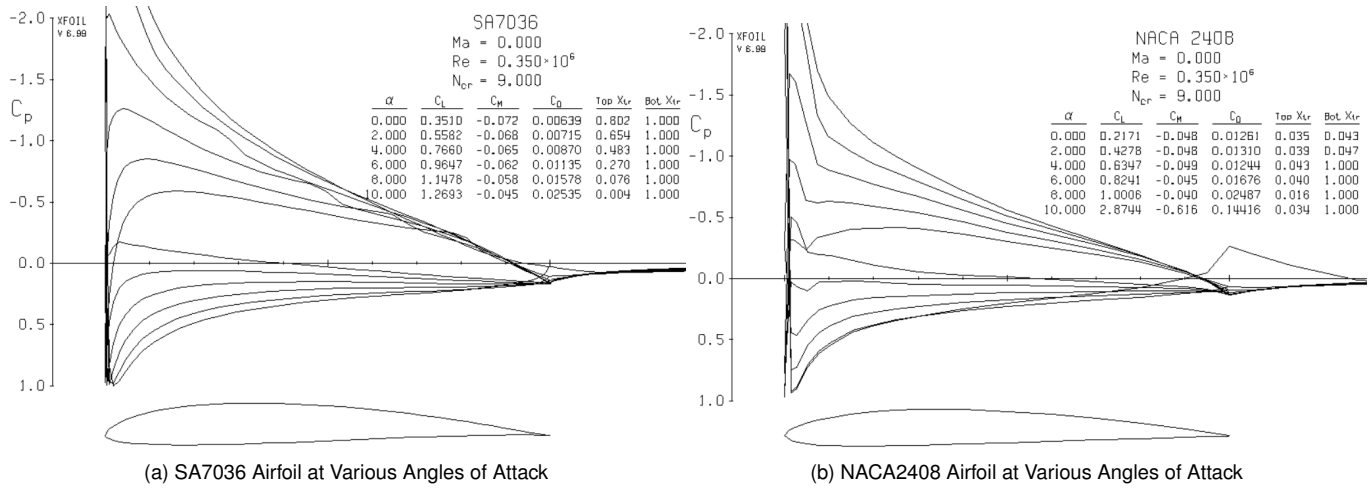
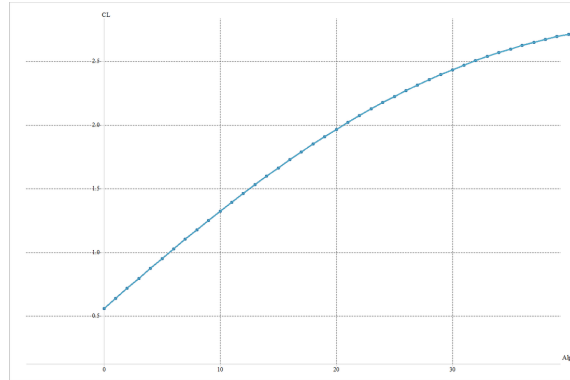


Figure 4.5.1: Airfoil Comparison

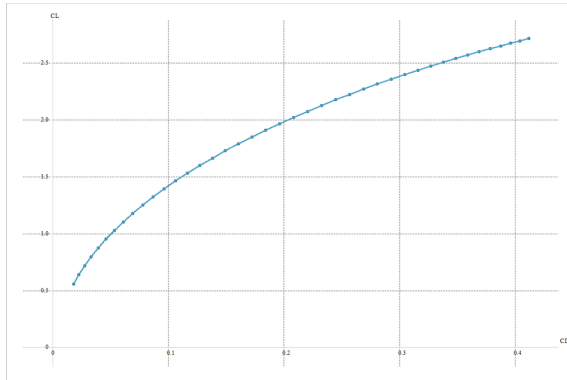
After analysis of the 2 airfoils, it was determined that the SA7036 had superior performance at low Reynolds numbers, necessary for take off, and had overall more lift and less drag.

#### 4.5.2 Drag Analysis

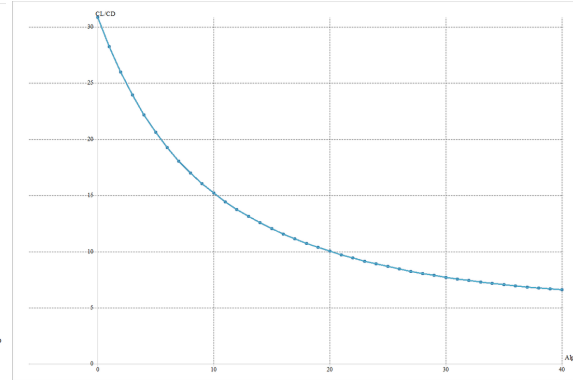
Given this year's mission, and the integration of the specific payloads, drag became a large design constraint. With a focus on mission 3, the team understood the importance of maximizing lift, and minimizing aircraft drag. To better understand limitations, the team analyzed the aircraft's major components including payload. Estimations for radome, attack stores, and fuselage were based on specific drag analysis via Solidworks Flow Simulation and XFLR5. Table 4.5.1 presents the coefficient of drag of each component, and their overall consideration and impact on mission 1 & mission 3 performance. During mission 3 with 12 attack stores, the aircraft flies at variable speeds 65-95 ft/s and encounters max drag due to payload, it was found that the maximal lift-to-drag ratio is 4.09 for the lowest velocity of 65 ft/s due to limitations of the propulsion system. While a low number the team expects this value to increase as attack stores are dropped and to be offset when introducing aerial  $C_L$  improvement techniques, reaching a  $L/D$  of 18 at max speeds. A visual representation of the lift and drag characteristics of the plane for mission 3 is given in figure 4.5.2.  $C_D$ ,  $V$ , and  $\alpha$  coefficients are averaged for the due to the variable flight speeds.



(a) Mission 3  $C_L$  vs  $\alpha$



(b) Mission 3  $C_L$  vs  $C_D$



(c)  $C_L / C_D$  vs  $\alpha$

Figure 4.5.2: Relationships between lift and drag characteristics for mission 3

Specific Case		Drag Analysis	
		Aircraft Component	$C_D$
Mission 1: $V = 80 \text{ ft/s}$ , $\alpha = 0^\circ$		Wing (1)	0.017
		Tail (2)	0.0005
		Fin (3)	0.00028
		Fuselage (4)	0.006
		Total	0.023
Mission 2: $V = 100 \text{ ft/s}$ , $\alpha = 0^\circ$		Aircraft Component	$C_D$
		Wing (1)	0.019
		Tail (2)	0.0006
		Fin (3)	0.0003
		Fuselage (4)	0.0075
		Radome (5)	0.0035
		Total	0.0309
Mission 3: $V_{\text{avg}} = 80 \text{ ft/s}$ , $\alpha_{\text{avg}} = 1.5^\circ$		Aircraft Component	$C_D$
		Wing (1)	0.02
		Tail (2)	0.00065
		Fin (3)	0.00028
		Fuselage (4)	0.007
		Payload (5)	0.104
		Total	0.13193

Table 4.5.1: Component Drag Analysis

## 4.6 Stability and Control

### 4.6.1 Static Stability

Utilizing XFLR5 the team was able to predict the aircraft's static stability. Due to a variation in CG, the team verified that its location was adequate to cruise for missions 2 and 3. The limits encountered based on the design produced a static margin of 10 percent and 22 percent, which occurred at 7 percent MAC and 19 percent. Iterations of the tail size and arm were conducted, to best satisfy Level 1 flying qualities as defined in MIL-F-875C. It was then found that for both the forward and aft CG that  $C_{m_a}$ ,  $C_{M_q}$ ,  $C_{l_p}$ , and  $C_{n_r}$  were negative while  $C_{n_b}$  remained positive, satisfying initial conditions for static stability.

Table 4.6.1: Forward CG limit static stability derivatives for mission 3.

$C_{X_u}$	-0.01	$C_{X_a}$	0.06	$C_{X_q}$	0.08	$C_{Y_b}$	-0.11	$C_{Y_p}$	0.01	$C_{Y_r}$	0.04
$C_{L_u}$	0	$C_{I_a}$	4.66	$C_{I_q}$	6.38	$C_{I_b}$	0	$C_{I_p}$	-0.65	$C_{I_r}$	0.05
$C_{m_u}$	0	$C_{m_a}$	-1.29	$C_{M_q}$	-4.38	$C_{n_b}$	0.02	$C_{n_p}$	-0.03	$C_{n_r}$	-0.01

Table 4.6.2: Aft CG limit static stability derivatives for mission 3.

$C_{X_u}$	-0.01	$C_{X_a}$	0.04	$C_{X_q}$	0.07	$C_{Y_b}$	-0.011	$C_{Y_p}$	0.01	$C_{Y_r}$	0.05
$C_{L_u}$	0	$C_{I_a}$	4.66	$C_{I_q}$	7.5	$C_{I_b}$	0	$C_{I_p}$	-0.65	$C_{I_r}$	0.04
$C_{m_u}$	0	$C_{m_a}$	-1.85	$C_{M_q}$	-5.6	$C_{n_b}$	0.02	$C_{n_p}$	-0.02	$C_{n_r}$	-0.01

#### 4.6.2 Dynamic Stability

Meeting the static stability requirements, the team determined it was safe to flight all mission. Despite of CG, angle of attack, and other flight derivations, the plane is expected to avoid stalling by using strong vortex generators and slits.

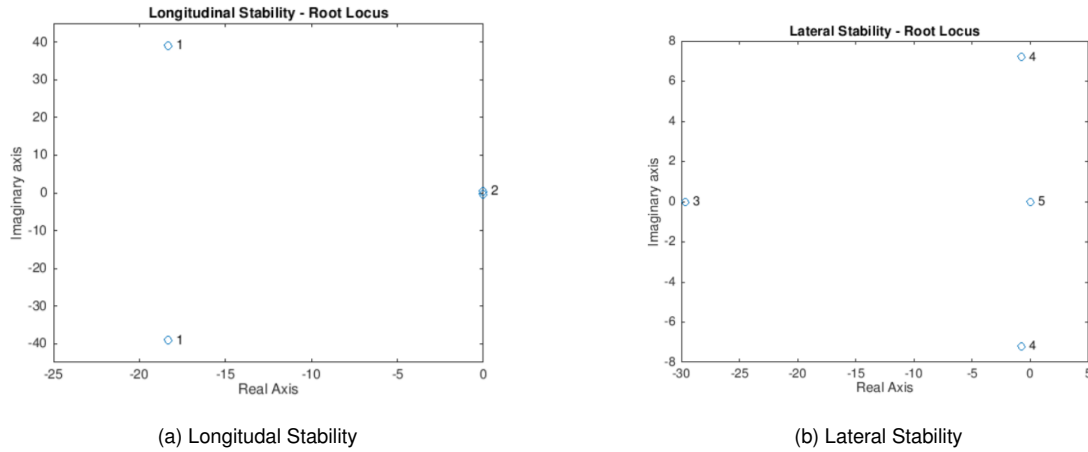


Figure 4.6.1: Stability analysis results

Figures 4.6.1 (a) & (b): 5 Modes of motion: (1) short period, (2) phugoid, (3) roll damping, (4) Dutch roll, (5) Spiral. The dynamic stability parameters for the forward and aft CG limits are shown in table 4.6.3.

Military Specification MIL-F-8785C was used as reference for stability characteristics. While there were certain modes such as phugoid where despite the low damping ratios, the flight test proved that the plane flew adequately.

Table 4.6.3: Dynamic Stability Parameters

#	Mode	$\zeta$		$\omega d$ [rad/s]		$\zeta_{\omega n}$		$\tau$ [s]	
		CG <sub>1</sub>	CG <sub>2</sub>	CG <sub>1</sub>	CG <sub>2</sub>	CG <sub>1</sub>	CG <sub>2</sub>	CG <sub>1</sub>	CG <sub>2</sub>
1	<b>Short Period</b>	0.436	0.453	55.16	43.67	-21.64	-17.64	0.37	0.43
2	<b>Phugoid</b>	0.036	0.026	0.377	0.446	-0.01	-0.01	101	105
3	<b>Roll damping</b>	-	-	-	-			0.23	0.21
4	<b>Dutch Roll</b>	0.091	0.094	6.63	5.43	-0.6	-0.49	12.7	15.3

#### 4.7 Transitioning to Stowed Configuration

The tail boom retraction mechanism utilizes the tail boom and an internal worm gear that actuates a collar on the boom, interfaced with ball joint struts on the wing. The worm gear slides the tail collar backward, actuating the wings rearward into the stowed configuration. This packaging configuration is the simplest to construct, however the actuation is large, requiring more material in the form of longer struts and worm gear that contribute to the total weight of the aircraft, requiring further optimization.

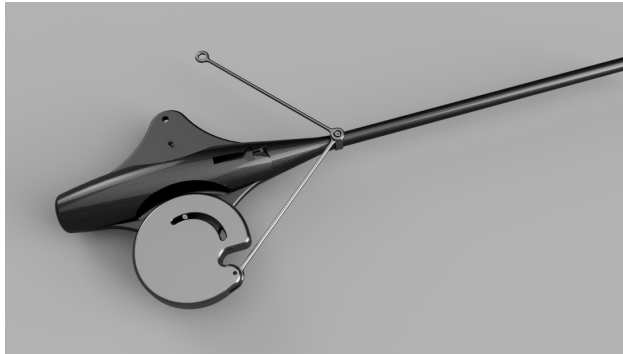


Figure 4.7.1: Considered Pivot Design Using Tail Boom Retraction

Upon further inspection, the team realized that if the wing pivots on a pin approximately 6" from the center-line of the plane, the pivot action can be actuated by the WHM, which consists of a tie rod end attached to both wings at a length  $L$  from the center-line, a pair of tie rod ends along the belly of the plane attached to a spring mechanism to lock the wings. After using relations of triangles with the offset hinge points, the team created the following formula relating the length of the tie rods to the travel distance of the sliding mechanism ( $\Delta x$ )

$$\Delta x = -L + 5.75 + \sqrt{L^2 - 32.0125} \quad (15)$$

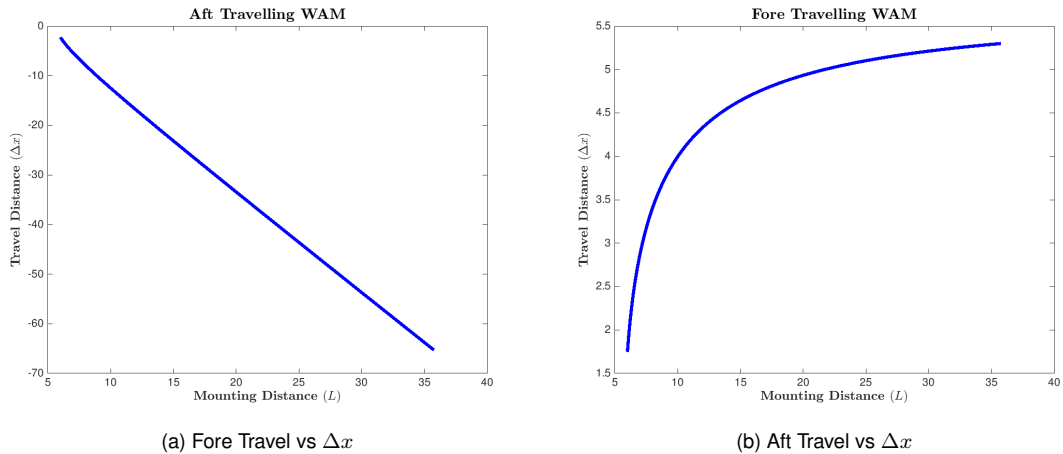


Figure 4.7.2: Aft & Fore Travel vs  $\Delta x$

Comparison of the Tail Boom Configuration and Fuselage Retraction options are shown in figure 4.7.2.

The fuselage retraction method had the lower  $\Delta x$ , making it superior due to the lower space requirement and the fact that it would (1) have less impact on the structure of the carbon fiber support rod for the tail, as the mechanism would require the rod to have a slit cut into it of length  $\Delta x$ , and (2) require much less material to actuate, saving weight on the aircraft.

## 4.8 Performance Estimates

Based on the aircraft specifications derived from the preliminary design study, the aircraft mission performance figures have been updated to reflect the aircraft aerodynamic and payload capabilities that will enable better flight times. Mission 1 is assumed to be completed within 5 minutes for a total of 1 point. Mission 2 is expected to be executed at 100 ft/s, with a continuous current discharge rate of around 17-19 amps. Mission 3 is conducted with a flight speed between 65-95 ft/s, with an average flight speed of 80 ft/s, utilizing variable speeds to keep the propulsion system operating at the most efficient loads. Mission performance is summarized in table 4.8.1.

<b>Mission Performance</b>	<b>Mission 1</b>	<b>Mission 2</b>	<b>Mission 3</b>
Attack Stores Launched	0	0	12
Weight (lbs)	3.3	3.7	5.9
Velocity (ft/s)	80	100	65-100
Lap Time (s)	42.45	36.23	42.89

Table 4.8.1: Mission Performance Estimates

## 5 Detail Design

The detailed design section builds upon conceptual and preliminary theoretical findings, providing a detailed overview of aircraft components, architecture, and capabilities that exceed mission requirements.

### 5.1 Dimensional Parameters Table

Geometric Data

<b>Overall Dimensions (in)</b>		<b>Fuselage (in)</b>	
Length	29	Total Length	17.3
Wing L.E X-Location	3.75	Tail Length	9.75
Landing Gear Location	F:1.25 R:12.25	Width	11.5
C. G. X-Location	7	Height	9

Wing (in)		Tail (in)	
Airfoil	SA 7036	Airfoil	NACA 0006
Span	90 in	Horizontal Tail Span	24
Chord	10 in	Horizontal Tail Chord	8
MAC	29%	Vertical Tail Span	9.33
Aspect Ratio	10.655	Vertical Tail Chord	6.25
Incidence Angle	0	Incidence Angle	0
Reference Area of Lift	800	Tail Arm	25

### Control Systems

Electronics & Controls		Motor	
Receiver	AR20310T	Model	T-Motor AT3520
Servo	Turnigy Metal Gear	Gearbox	Direct Drive
Battery Model	HRB 50C 4500mAh	kV	550
Internal Resistance	0.010	Power Rating	850 W
Cell Count	6S1P	No-Load Current	0.132 A
Pack Voltage	22.2 V	Internal Resistance	0.087 Ω
Pack Weight	1.2 lbs	Weight	0.463

## 5.2 Structural Characteristics and Capabilities

In this section, structural characteristics and load capabilities of the core aircraft components are detailed. All aircraft components are thoroughly tested to be able to withstand the aerodynamic and inertial forces required to successfully complete missions  $M_1 - M_3$  as designed.

### 5.2.1 Fuselage and Frame

The split wings of the aircraft were designed to be connected directly to the center frame of the fuselage. This effectively split the fuselage into upper and lower sections. The lower section is responsible for housing all heavy electronics that need cooling (ESC, Batteries), and the upper portion holds all electronics for avionics control. The tail boom is also connected to this center CFRP plate. The central CF has a thickness of about 0.5 in, and is completely molded using CFRP manufacturing techniques.

The fuselage is a complex monocoque design created from a four part female mold. It was created from two sheets of carbon fiber in a polymer matrix with a layer of 0 degree thread followed by a 45 degree thread layer for

added strength. This laminated shell serves to be a mounting location for all electronics, radome directly above the CG, and meets the aerodynamic needs of the design. Furthermore, it provides complimentary structural support for the central frame.



Figure 5.2.1: Internal and External View of the Fuselage

### 5.2.2 Wing

A tried and true method for wing construction was used for this year's plane. The wing was broken into discrete sections by cross sections of the airfoil, joined together with one spar, three to four stringers, and a continuous leading and trailing edge. This hollow shape was then wrapped in a heat shrink polymer. The majority of the internal volume of the wing is void, keeping the wing lightweight, while the leading and trailing edges maintain the exact dimensions of the airfoil selected. Material selection was broken down into 2 separate groups; Balsa wood and CFRP. Rib and leading edge material are the difference between the 2 groups, where the leading edge and ribs will be balsa wood for the balsa wood and CFRP group, versus an all CFRP design.

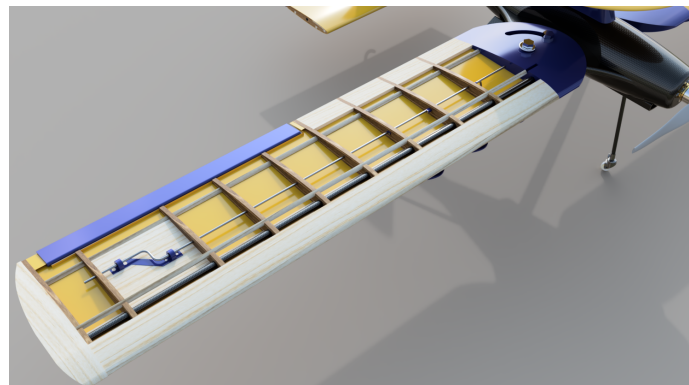


Figure 5.2.2: Internal Wing Structure

To maintain a low weight and high strength for the wing, the structure consists of hollow ribs, a hollow composite spar, solid stringers, a thin plate for the leading and trailing edges, and a thin skin. The design can be seen in figure 5.2.2. The ribs consisted of a truss-like internal structure, while the physical layout of the rib was either a composite-foam-composite sandwich, or a composite laminate. The latter being used towards the wing root to provide all the necessary strength in shear and bending. This overall internal structure provides the necessary rigidity and strength, while remaining as lightweight as possible. The composite-foam-composite sandwich prevented buckling and allowed mounting locations for servos and internal mechanisms. The leading and trailing edges of the ribs were wrapped in thin plate of carbon fiber or balsa wood. This kept the heat shrink polymer skin from deforming past the required airfoil shape and retained the desired aerodynamics of the wing.

The spar took the shear and bending forces from the wing and transferred them to the main wing plate, while the stringers prevented torsional loads from deforming the wing shape.

### 5.2.3 Tail

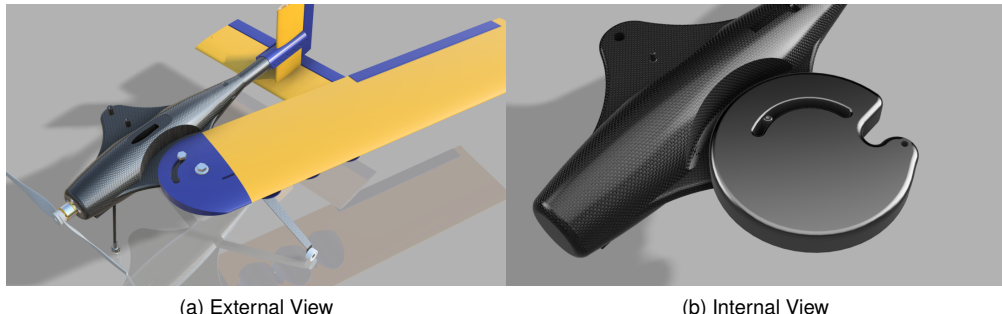
The tail uses the same architectural design of the wings, with the exception of airfoil and size requirements.

## 5.3 Subsystem Design and Integration Architecture

All payload subsystems were built to be completely modular to fully meet GM requirements. The design architecture is detailed in the following subsections, with models provided to aid visualization and understanding of the methodology behind the subsystem design and architecture of each component.

### 5.3.1 Pivot Wing Mechanism

The fore/aft travel pivot wing mechanism was optimized to no longer require the strut assembly for extra strength. This optimization was the result of better CF manufacturing techniques, increasing wing and central fuselage rigidity. As such, the team decided to utilize a servo actuated pivot wing mechanism. A high 23kg-cm torque servo was selected to directly drive each wing into flight configuration, embedded within the CF subframe. The wings lay on the CF sub-frame and are tightened down using an internal mechanism embedded within the wings that ensures full pressurized contact between the wings and CF subframe. [3]



(a) External View

(b) Internal View

Figure 5.3.1: Servo Actuated Pivot Wing Mechanism

### 5.3.2 Attack Stores

The plane was designed to hold six attack stores on each wing (three shown in figures). Each wing has its own assembly for controlling the attack stores. Each attack store is attached to a custom mount comprised of polystyrene foam due to its low weight and ease of construction. The mount is secured to the wing permanently with screws. The attack stores are held in place to the mount by an elastic band. One end of the band is securely attached to the permanent mount and the other end is held securely by a release pin, shown in figure 5.3.2.

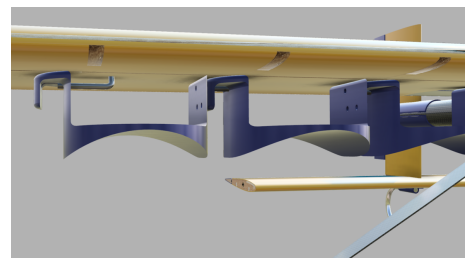


Figure 5.3.2: Release Pin Representation

The attack store release assembly consists of 2 ft of 1/16 inch rod that is fed laterally through the ribs inside of the wing. Three short release pins (one for each attack store) varying in size by 3/4 inch length are welded to the main rod. These pins have three strategically placed 90 degree bends that act as the release mechanism for holding and releasing the elastic band, ultimately ejecting the attack store. One end of the thin rod is attached to a positional rotation servo with a custom made 3D printed horn. The other end of the rod is supported by a 3D printed linear-motion guide, shown in figure 5.3.3 (b). The linear movement of the thin rod is controlled by the servo with the custom horn.

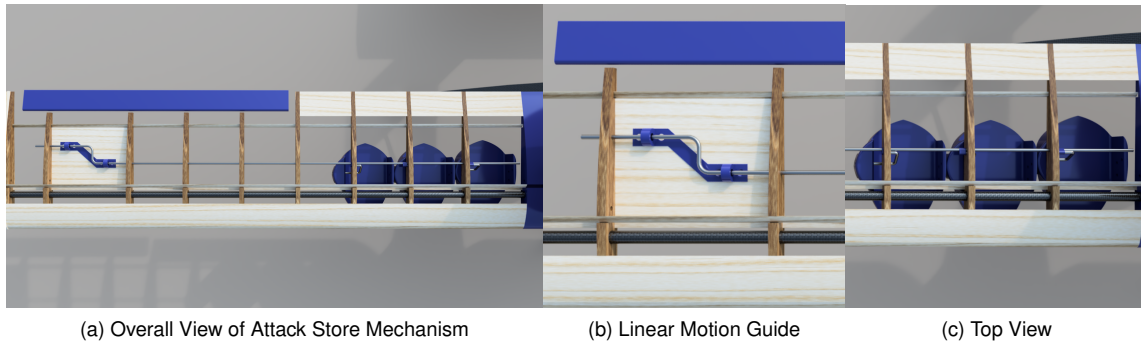


Figure 5.3.3: Attack Store Design

The servo maintains four discrete positions based on state of the attack store configuration. It's rotation has a range from 45 to 135 degrees with the  $x$  direction being lateral with the wing. Once armed, the servo begins at position one, 45 degrees. The servo then rotates 30 degrees between each of the four static positions in the direction of increasing angle. Each 30 degree rotation shifts the rod 3/4 of an inch in a lateral, linear fashion causing the attached holding pins to shift with the assembly.

The shortest pin is on the outermost attack store of each wing, the medium pin is next to the outermost, and the longest pin is the closest to the fuselage. After the first 3/4<sup>th</sup> inch lateral shift of the assembly, the shortest, outermost pin releases its elastic band, therefore deploying the attack store. Each subsequent lateral shift in the assembly releases another attack store. This attack store configuration can be linearly scaled to carry as much as 12 stores.

### 5.3.3 Plug in Radome

Two things were essential to the design of the radome. It needed to be modular for easy installation and drag needed to be kept to a minimum while still meeting the constraints. Built into the fuselage, is a notch with spring detents that mesh with a 3D printed "plug", glued to the radome mount, allowing the entire radome structure to be removable. The radome and its mounting post was made primarily of polystyrene foam Monokote to reduce parasitic drag, symmetrical shaped to reduce drag to negligible amounts at

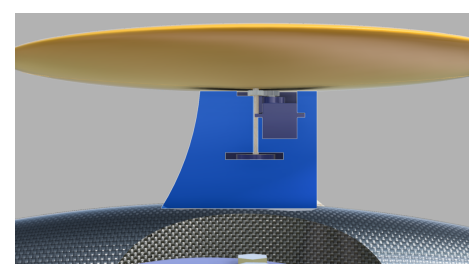


Figure 5.3.4: Final Design Radome Configuration

an angle of attack of 0 degrees, during cruise flight. On top of the radome some pattern will be created to indicate turning.

Inside the post is a cut out for a modified servo and the axle made from a wooden dowel which mounts the radome to the post. The servo was modified by removing the limiter turning it into a 360 degree rotating servo. Attached to both the 360 degree servo and the axle are 3D printed gears that transfer the rotation of the servo to the axle allowing the radome to turn. A detailed render of the radome configuration is presented in figure 5.3.4.

#### **5.3.4 Electronics Bay**

All electronics are housed in the lower half of the aircraft fuselage, including the batteries. This was done to strategically locate the majority of mass below the center of lift for the wing, inducing stability effects found in high-wing designs. Furthermore, the lower half of the fuselage is designed to have high airflow rates to keep mission critical components cool. The fuselage is designed to guide "clean" air through the electronics bay, inducing a slight swirl in the flow, ensuring that all components are convectively cooled and the inlet/outlet has the least drag contribution possible.

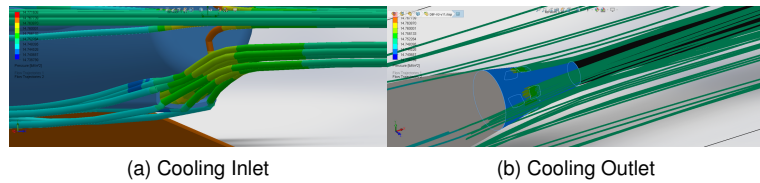


Figure 5.3.5: Electronics Bay Cooling

#### **5.3.5 Propulsion System**

For the propulsion system, the motor was mounted to the direct front of the fuselage using a plywood mounting plate and associated bulkhead to connect to the rest of the supporting fuselage structure and main wing plate. The ESC was mounted in a separate bay with direct airflow across it from a scoop on the fuselage. Wiring and arming plugs were mounted on the exterior of the fuselage, just behind the motor. Battery locations are on the bottom of the main wing plate, and wiring subsequently went through the main wing plate in a series of small holes. This year, the team decided to not have an individual location for batteries, but rather a range of locations for the batteries so the CG of the plane can be adjusted for each of the missions, as well as the number of batteries.

Propulsion Components	Mission 1		Mission 2		Mission 3	
	Description	lb	Description	lb	Description	lb
<b>Motor</b>	Cobra C-3520 980 kV Brushless	0.463	Cobra C-3520 980 kV Brushless	0.463	Cobra C-3520 980 kV Brushless	0.463
<b>Receiver</b>	Spektrum AR20310T	0.132	Spektrum AR20310T	0.132	Spektrum AR20310T	0.132
<b>ESC</b>	YGE 60A	0.0772	YGE 60A	0.0772	YGE 60A	0.0772
<b>Receiver Battery</b>	Venom 1200mAh 6V	0.249	Venom 1200mAh 6V	0.249	Venom 1200mAh 6V	0.249
<b>Propulsion Battery</b>	Elite 1500mAh (19)	1.21	Elite 1500mAh (19)	1.21	Elite 1500mAh (38)	1.21
<b>Total Weight</b>	2.13 lb		2.13 lb		3.35 lb	

Table 5.3.1: Propulsion Components

### 5.3.6 Landing Gear

The design of the landing gear was heavily influenced by the restrictions on landing gear positioning. The plane was designed to be a total of 27 inches in length, and the rules required a tail hook to be mounted to the aft end of the plane, so conventional landing gear was out of question. The team turned towards a tricycle landing gear, and guided the design according to the sketch in figure 5.3.6. [2]

Some variations occurred from the specifications in 5.3.6 for this competition, due to the ramp the plane will launch from. The rear landing gear position is used to ensure the elevator will be able to lift the front of the plane off the ground for normal flight. However, in the scope of the competition, it is not necessary to bring the front landing gear off the ground using the elevator. This allows the team to move the rear landing gear further back to account for a CG shift when the wings are stowed. The following graph shows the total change in CG from its current position on the aircraft when the wings are stowed at an angle such that the wing tips are each 1 in from the edges of the 3 ft box.

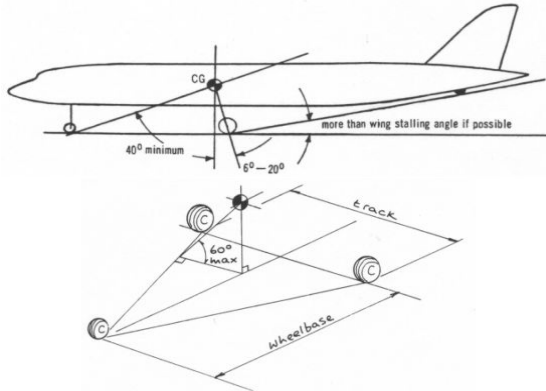


Figure 5.3.6: Landing Gear Stability [2]

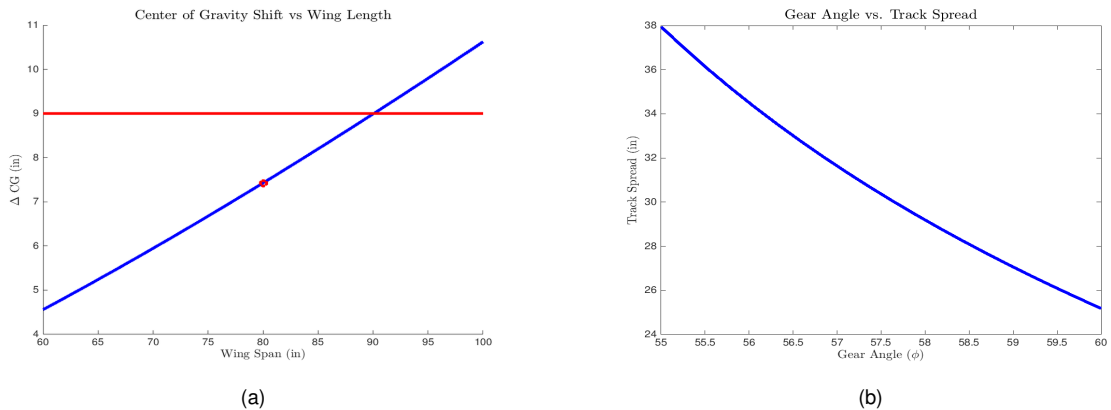


Figure 5.3.7: Landing Gear Design Constraints

The track of the landing gear was mainly constrained by the roll stability of the plane in taxi. The minimally stable angle is 60 degrees, and the following graph was used to find the total track width needed to keep the plane safe while on the ground. The team decided on a track width of 32 in derived from figure 6.2.1, to add extra stability and account for error during manufacturing. Figure 5.3.8 presents the current design of the landing gear.

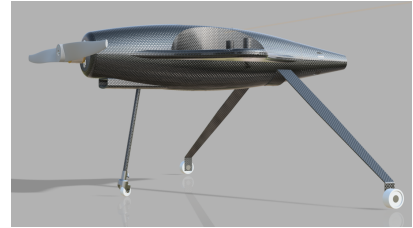


Figure 5.3.8: Landing Gear Design

## 5.4 Weight and Mass Balance

Given this year's constraints, specifically the utilization of the inclined ramp limited the aircraft's weight. The aircraft's weight for mission's 1,2, and 3 was found to be 3.3, 3.5, and 5.9 lbs. These calculations were found satisfactory as covered in section 3.2. For all missions, the battery was utilized to accommodate for the CG location in reference to the neutral point. This kept the design of the Static Margin under control, and ensured safe flights. In the following table all the aircraft CG components are labeled. Note all values are in reference to the aircraft's center-line, and the leading edge of the wing.

Aircraft Component	Weight		X		Y		Z	
	(lb)	(kg)	(in)	(cm)	(in)	(cm)	(in)	(cm)
M <sub>1</sub>	3.30	1.50	1.34	3.40	0	0	-0.20	-0.51
Wing	1.10	0.50	2.90	7.37	0	0	-0.13	-0.33
Elevator	0.07	0.03	19.63	49.86	0	0	-2.93	-7.44
Fin	0.03	0.01	19.63	49.86	0	0	0.50	1.27
Motor	0.57	0.26	-6.70	-17.02	0	0	0	0
Propeller	0.06	0.03	-6.90	-17.53	0	0	0	0
Battery	1.20	0.55	-3.0	-7.62	0	0	-0.70	-1.78
Front Fuselage	0.19	0.09	2.90	7.37	0	0	-0.40	-1.02
Boom Fuselage	0.08	0.04	8.75	22.23	0	0	-0.40	-1.02
M <sub>2</sub>	3.5	1.60	1.34	3.40	0	0	-0.20	-0.51
Payload	0.20	0.09	4.3	10.92	0	0	1.70	4.32
M <sub>3</sub>	5.90	2.68	0.68	1.73	0	0	-1.03	-2.62
Battery	2.40	1.10	-3.0	-7.62	0	0	-0.50	-1.27
Payload	1.375	0.63	2.90	7.37	0	0	-3.2	-8.13

Table 5.4.1: Weight and balance table for flight missions

## 5.5 Flight and Mission Performance

The final predicted mission performance of the aircraft was derived using DTS\_Cat, presented in table 5.5.1. Corresponding mission scores based on predicted performance are also included in 5.5.1.

Performance Parameter	Mission 1	Mission 2	Mission 3
CD	.019	.021	.318
CL - Max	2.07	2.07	2.6
CL - Cruise Speed	0.54	0.54	0.60
(Lift/Drag) - Max	18.47	17.94	4.09
(Lift/Drag) - Cruise Speed	14.35	14.35	5.184
Rate of Climb (ft/s)			16
Speed - End of Ramp (ft/s)			24
Wing Loading (lb/ft <sup>2</sup> )	0.594	0.63	1.062
Cruise Speed (ft/s)	80	100	85 <sub>avg</sub>
Stall Speed (ft/s)			24
Battery Weight (lb)	1.2	1.2	2.4
Total Weight (lb)	3.3	3.5	5.9
Mission Score			

Table 5.5.1: Predicted Aircraft Performance

## 5.6 Drawing Package

The following five pages contain the plane's 3-view, wing assembly, attack store assembly, radome mechanism, and stowed wing configuration drawings.

## 6 Manufacturing Plan and Process

Considering that the aircraft geometry is complex, the team realized that a combination of different manufacturing techniques had to be used in order to construct the aircraft accurately and in a timely manner.

### 6.1 Manufacturing Methods Considered

No one manufacturing method was adequate enough to construct the aircraft based on design requirements put in place by the Design Engineers. As such, multiple manufacturing methods were investigated for possible use when constructing the aircraft.

- **3D Printing:** This additive manufacturing process granted the team the ability iterative improve and test various subsystem components. The main uses were:
  - Printing aerodynamically complex aerodynamic shapes, such as a fuselage mold for CF vacuum bagging
  - Generating custom guides to allow a linear range of motion of the rod used in the attack store mechanism assembly
  - Rapid prototyping of different aircraft parts
- **Balsa Wood Construction:** Balsa wood was a favorable material due to its high strength to weight ratio, as well as its low density. It is a light material with high stiffness. Balsa's low density allowed it to be easily cut using laser cutters at efficient rates. These characteristics made it a favorable material for wing ribs, since it provides minimal weight, flexibility and strength. However, it did not provide the necessary strength for many key loading structures.
- **Foam:** The team has built the prior competition aircraft 80% out of high density polystyrene foam. While it did provide great structural rigidity for the weight, this manufacturing procedure results in additional weight due to a minimum thickness that the foam needs to have to be structurally competent, making it not as attractive compared to other options. Furthermore, shaping the foam has proven to be time intensive.
- **Vacuum Bagging Composites:** The advantages that comes with the use of composites, such as carbon fiber and fiberglass, are greater tensile strength and lighter weight. In prior years, composite material use was limited to carbon fiber rods for structural reinforcement. Due to newly acquired vacuum bagging techniques, this form of manufacturing can be advantageous for key structural components that are under constant high loading.

### 6.2 Manufacturing Process Selected

The team identified that a majority of the manufacturing methods considered are applicable for use in constructing the aircraft. The most optimal manufacturing method was to use cross-disciplinary manufacturing.

- **Wing and Tail:** The aircraft wing and tail was primarily made using balsa wood to minimize weight. Each side of the wing was made around a carbon fiber main spar, which supported the laser cut balsa ribs to give

the wing strength and shape to the airfoil. The ribs were attached to each other with additional balsa wood beams ruining the length of the structure, and fastened with the use of cyanoacrylate (CA) glue where the ribs and the spars intersected. After the internal structure is finished it is covered in monokote to maintain the airfoil throughout the wing.

- **Fuselage Structure:** With the team's capability of vacuum forming, it was selected to be the main method for manufacturing the fuselage's complex geometry. The fuselage was comprised of carbon fiber and foam composites for its lightweight and rigid properties. The outer shell of the fuselage is two layers thick of carbon fabric with the first layer angled at 45 degrees and the second layer being 90 degrees. This practice allowed for extra tensile strength and stiffness without adding any extra material and weight. The mold for the fuselage was made out of 3D printed polylactic acid (PLA) and allowed for the precise dimensions required in manufacturing. Inside the fuselage, the wing support used two carbon fiber plates with a thick layer of polystyrene foam creating a composite-foam-composite sandwich. The carbon fiber plates were made with 3 layers of carbon fiber with staggered threading angles. All 4 carbon fiber parts were created using female molds, 4 hour cure epoxy resin, and were all vacuum formed for at least 4 hours.
- **Pivot Wing Mechanism:** The pivot wing mechanism consisted of pre-made nylon CNC parts, and composite materials that attach to the wing and the main wing plate. These pieces were designed for large amount of stress at the pivot point while transferring load from the wings to the fuselage. Having the ability to rotate the wing through the use of a 360 degree high torque servo inside the fuselage that drives the mechanism of the wing actuation and locking. The parts were made with high tolerances to minimize wing flutter and ensure structural rigidity for flight during all missions.
- **Attack Store Mechanism:** Almost all parts used by the attack store mechanism have been developed using 3D, with over 10 different iterations printed to ensure that the geometry and parts exceed mission and structural requirements.

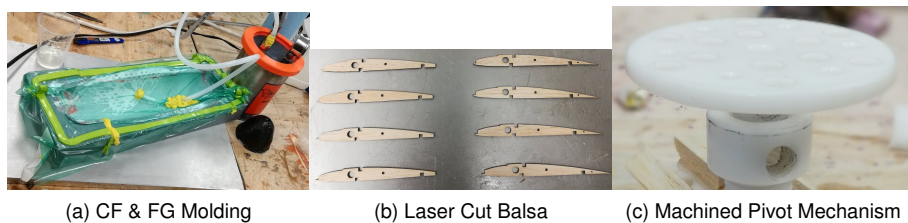


Figure 6.2.1: Multiple Manufacturing Methods Utilized

### 6.3 Manufacturing Milestone Chart:

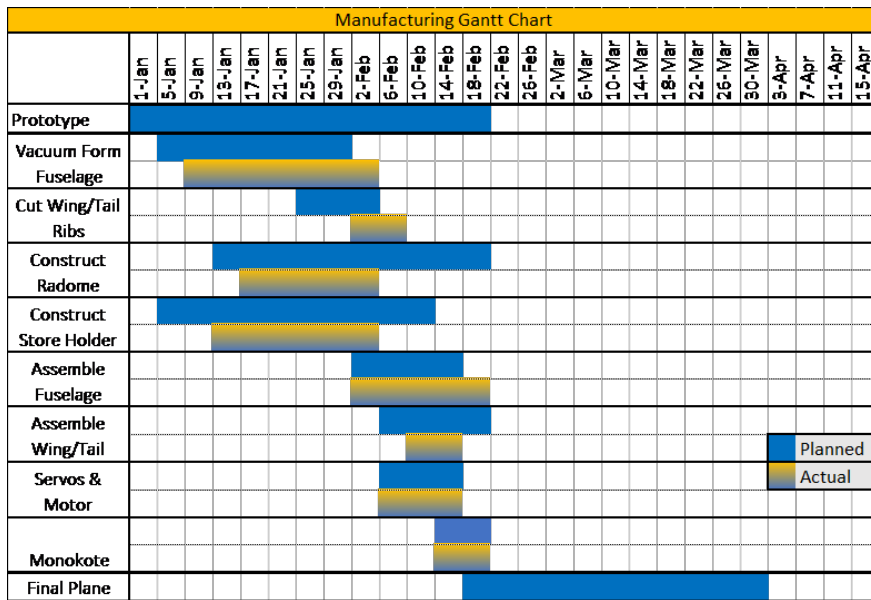


Figure 6.3.1: Manufacturing Milestone Chart

## 7 Testing Plan

All components in the aircraft were tested and vetted carefully and thoroughly. Special attention was given to key structural components and the propulsion system, if those fail then it would result in an immediate setback in the team's ability to continue with the competition. The testing plan is presented in figure 7.0.1.

Test Plan - Current Date: 02/2019	September	October	November	December	January	February	March	April
<b>Subsystem Testing</b>								
Fuselage Testing	Planned	Planned	Planned	Planned	Planned	Planned	Actual	
Flight Surfaces Testing	Planned	Planned	Planned	Planned	Planned	Planned	Actual	
Pivot Wing Assembly Testing		Planned	Planned	Planned	Planned	Planned	Actual	
Attack Store Assembly Testing			Planned	Planned	Planned	Planned	Actual	
Radome Assembly Testing				Planned	Planned	Planned	Actual	
Propulsion System Testing				Planned	Planned	Planned	Actual	
Ground Mission Practice/Testing					Planned	Planned	Actual	
<b>Flight Testing</b>								
Proof of Concept Flights				Planned	Planned	Planned	Actual	
Preliminary Design Flights					Planned	Planned	Actual	
M3 Six Attack Store Flights						Planned	Actual	
<b>Final Aircraft Flight Testing</b>								
M1 Performance							Planned	Planned
M2 Performance			Planned:				Planned	Planned
M3 Twelve Attack Store Performance		Actual:					Planned	Planned

Figure 7.0.1: Testing Plan

## 7.1 Test Objectives

- Propulsion:
  - Ensured that the selected motor can effectively carry the aircraft and payload while ensuring high performance when in flight
  - Ensured that the propulsion system can maintain a full load until battery capacity reaches critical levels in flight and in static bench situation
  - Demonstrated that the propulsion system can safely meet all power demands from the pilot
- Aerodynamics:
  - The structure was simulated in Solidworks to ensure minimum drag coefficients were produced
  - Flight tests were executed to verify in flight stall characteristics over tall grass at the UC Merced Vernal Pool Reserve
- Performance:
  - Flight tests were conducted to validate theoretical estimates from DTS\_Cat vs real world flights
  - Ramp takeoff tests were conducted to ensure that the aircraft is able to reliably take off from the competition ramp
- Payloads:
  - Attack store restraint systems were tested to ensure that only one store is launched at a time when commanded by the pilot or co-pilot
  - Radome was tested to ensure that it is capable of spinning and halting spinning motion on pilot command
- Wing:
  - Structural wing tip tests were carried out, along with in-flight aerobatic moves to ensure that the wings were capable of sustaining loads higher than the normal operating range
  - Failure/deflection points predicted by Solidworks Structural Simulation were verified using wing tip tests
  - Wing pivot mechanism was tested to ensure that no separation/failure occurs when the aircraft is subjugated to the prior two tests above
- Fuselage & Frame:
  - Bending and torsional testing was conducted to ensure that the fuselage and frame remained stiff in all situations

## 7.2 Subsystem Testing

### 7.2.1 Propulsion Testing

The propulsion system was tested statically using a custom built Arduino prop/motor test bench and dynamically tested in flight. During flight tests, the propulsion system provided more than adequate thrust to take off within the 10 ft ramp, proving the theoretical calculations met or exceeded takeoff requirements. Propulsion tests also

consisted of battery loading stress tests. Fully charged NiMH batteries were drained by the selected propulsion configuration and monitored at 100% throttle until they were completely depleted to their nominal 1.2 V. These tests validated the simulation and electronics engineers' calculations, ensuring adequate endurance for mission 3. Furthermore, the propulsion system was able to maintain in-flight full throttle conditions for 5 minutes, this demonstrated reliability in conditions that required extended maximum throttle input. Peak power recorded was 704 W, at 32 A and 22 V power draw in 3000 mAh configuration, for the launches including up to 12 attack stores in weight.

### **7.2.2 Structural Testing**

In-air aerodynamic forces were simulated utilizing tests conducted by subjugating the aircraft to simulated loads using weights, ensuring that the pivot mechanism and wing are both able to withstand the forces. The two key structures tested where the wing, pivot mechanism, and frame. Simulation studies were done using Solidworks Structural Simulation to ensure that theoretical characteristics of the wing meet or exceed mission requirements. To guarantee that the aircraft passes flight tech inspect and verify theoretical simulations, a wing tip test was performed to ensure that it could support its maximum weight with all components and payload included at 5G loads.

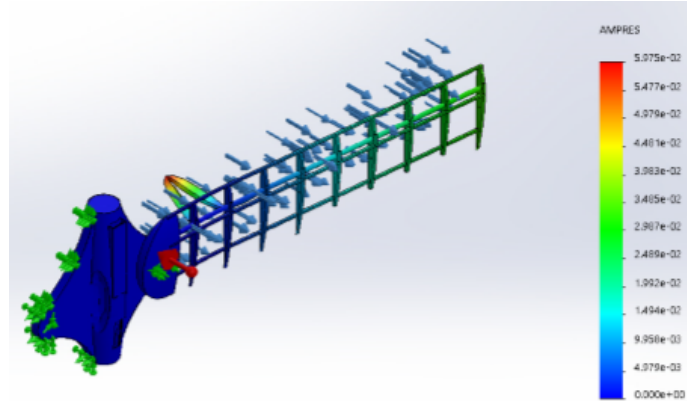


Figure 7.2.1: Structural Theoretical Testing

### **7.2.3 Subsystem Testing: Radome**

A fixed non-rotating version of the radome with the required dimensions was tested in flight on our prototype aircraft to see if there were any significant effects on flight characteristics. Further tests were conducted to simulate the loads applied to the radome and mounting structure in a similar way to the wing tip load test. A 2.5 kg weight was attached to the mounting plug and the entire assembly was lifted by the radome to ensure the adequate strength of our components and the ability for the radome to spin under load.

### **7.2.4 Subsystem Testing: Attack Stores**

Repetitive testing was done to ensure consistent, reliable operation of the mechanism. The attack store testing was successful with results that concluded in high confidence in the assembly. Initial testing performed on this assembly consisted of a tension test on the holding pins. These pins were able to withstand tensions far exceed-

ing the tensions expected of an elastic band around an attack store without issue. Because of the simplicity of the attack store mechanism chosen, there was no expected changes in dynamics when the mechanism was placed inside the wing. In addition, the rotating wing was not a concern for this assembly. Different effects of acceleration due to maneuvering and tilting of the plane have been considered, but were not expected to cause conflict with this design. Other considerations were the flexing of the wing when experiencing turbulence or during takeoff or landing. To account for any possible slippage of the holding pins, the length of travel required to release each holding pin to  $3/4^{th}$  inches was increased.

### **7.2.5 Takeoff Ramp Testing**

The takeoff ramp for the competition is 10 ft long at an angle of 5 degrees. This means that the end of the ramp is approximately 10 inches off the ground. A ramp simulating takeoff conditions was constructed using plywood and some basic hardware. It was a two piece that connect with screws, quick disassembly for quick transportation. The end of the ramp had a 10 inch section attached with a hinge so that it could be opened for use and closed for transport and storage. The ramp was used for every test flight to ensure that the plane was able to take off within the given parameters of the competition rules.

## **7.3 Flight Test Schedule and Plan**

Flight tests were conducted for each prototype to determine if aircraft performance met expectations. This was an important process in the production of our aircraft that provided insight for necessary modifications to the design. Each flight test was conducted with objectives that would improve the final design of the aircraft. Flight data was collected using an open-source autopilot, the 3DR Pixhawk. 3DR's open-source platform allows implementation of custom made software, simplifying the collection of detailed flight dynamics. Data collected was then processed using MATLAB to create graphs that help visualize how the plane performs in flight. In table 7.3.1, are the scheduled flight dates with set objectives. Tests were performed at the University of California, Merced Vernal Pools.

<b>Flight</b>	<b>Date</b>	<b>Objectives</b>
1	11/10/18	- First flight test on ramp - Determine if aircraft can takeoff based on DTS_Cat predictions
2	11/20/18	- Test and insure landing gear and forward/backward tip dynamics are adequate - Test geometry of the wing
3	11/28/18	- Test radome aerodynamic influences - Test stall characteristics
4	12/15/18	- Further test stall characteristics
5	1/13/19	- Test propulsion system adequacy
6	2/10/19	- Test mission 3 performance with full payload
7	2/30/2019	- Test third prototype with improved flight dynamics
8	3/10/2019	- Test final aircraft for further incremental changes

Table 7.3.1: Flight Test Dates and Objectives

## 7.4 Flight Checklists

A preflight checklist was used and conducted before each test to ensure the plane is secure and safe to fly (see table 7.4.1). This allowed for efficient gathering of data and minimized possible factors that would create errors. Further performance results will be discussed in the following section. Failure to pass the preflight and aircraft checklists (see table 7.4.2) results in the reassessment of the aircraft.

Components	Task
Fuselage (internal)	<input type="checkbox"/> Secure connections to Receiver <input type="checkbox"/> Secure connections to ESC <input type="checkbox"/> Check CG
Fuselage (external)	<input type="checkbox"/> Close and secure all access points <input type="checkbox"/> Prep landing gear for takeoff <input type="checkbox"/> Check CG
Pilot's Checklist	<input type="checkbox"/> Arm ESC <input type="checkbox"/> Complete control Check <input type="checkbox"/> Motor run up <input type="checkbox"/> Make Go/ No-Go Decision

Table 7.4.1: Preflight Checklist

Components	Items to inspect
Motor	<input type="checkbox"/> Motor mount is secured and fastened <input type="checkbox"/> Motor mount is damage and debris free <input type="checkbox"/> Prop is fastened correctly and secure <input type="checkbox"/> Prop is debris and damage free
Fuselage	<input type="checkbox"/> Batteries are connected and secured <input type="checkbox"/> Servos are connected and secured <input type="checkbox"/> Receiver connected properly and secured <input type="checkbox"/> ESC is connected properly and secured <input type="checkbox"/> Horns are fastened and in position <input type="checkbox"/> Close and secure all access points <input type="checkbox"/> Check CG
Wings	<input type="checkbox"/> Pivot mechanism works properly <input type="checkbox"/> Wings in proper starting position <input type="checkbox"/> Attack stores are damage and debris free <input type="checkbox"/> Payload(s) secured (if applicable) <input type="checkbox"/> Wings are secured to mounting point <input type="checkbox"/> Free of tears, damage, and obstruction
Control surfaces	<input type="checkbox"/> Servos are connected properly <input type="checkbox"/> Ailerons function properly <input type="checkbox"/> Elevator functions properly <input type="checkbox"/> Stabilizer functions properly <input type="checkbox"/> Can move without obstruction <input type="checkbox"/> No obvious damage
Landing Gear	<input type="checkbox"/> Landing gear is securely fastened <input type="checkbox"/> Wheels spin without obstruction <input type="checkbox"/> Check CG
Attack Stores (if applicable)	<input type="checkbox"/> Servo horns in correct position <input type="checkbox"/> Servos release on command <input type="checkbox"/> Holding mechanism can open <input type="checkbox"/> Payload(s) secured <input type="checkbox"/> Check CG

Table 7.4.2: Aircraft Inspection Checklist

## 8 Performance Results

The team implemented an autopilot system into the aircraft that utilized open source ArduPilot software and 3DR Pixhawk hardware to gather all key mission performance data. [5] Mission Planner by Micheal Osborn & the ArduPilot developer team was used as the Ground Control Station. [5] All propulsion and aerodynamic characteristics where derived from in-flight data. Pixhawk subsystems and modules where thoroughly calibrated. Note, due to unforeseen shipment issues, the aircraft was tested using a single 19 cell NiMH battery pack. The aircraft was designed to use two 19 cell NiMH battery packs wired in parallel to complete mission 3. To compensate for this, the team used only six attack stores payload weights. Full mission performance testing for mission 3 is scheduled to take place as soon as the ordered NiMH cells arrive.

### 8.1 Demonstrated Performance of Key Subsystems

**Ramp Launch:** The aircraft launch performance was tested and using a ramp built to mission launch specifications. The aircraft was successfully able to launch with 100% reliability. Detailed takeoff parameters are presented in table 8.1.1.

Takeoff Data	Data Derived from Mission Planner
Takeoff Velocity	22 ft/s
Battery Cell Count	19S at 25V
Power	364 W
Weight	4.12 lbs
Thrust	4.3 lbs

Table 8.1.1: Takeoff data

**Propulsion:** Thorough in-flight propulsion testing was conducted by running the propulsion system at max throttle until the batteries where completely depleted. DTS\_Cats predicted that total flight time at max throttle to be 6.5 minutes at a constant 340 W power draw. Peak amperage drawn was 20 A and minimum  $V_{sag}$  was 18.2 V.

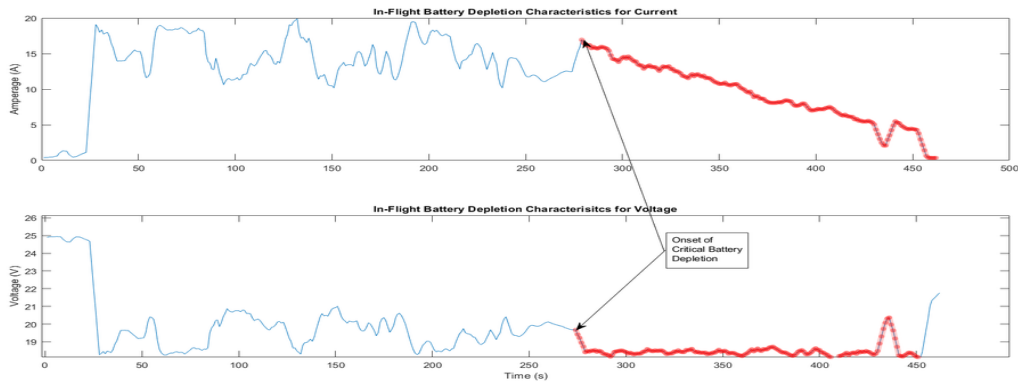


Table 8.1.2: In-Flight Battery Performance

To account for circumstances where full throttle would be necessary, such as slower than expected mission 3 performance due to pilot error, the team chose to perform the testing at max throttle. This allowed the team to model an equation that determined the onset of critical battery depletion in-flight for the Turnigy 1500 mAh NiMH battery cells.

$$\Delta C_{\text{critical}} = -7.5932x + 1628.5 \quad (16)$$

Equation 16 models the critical depletion onset and is implemented into the team's telemetry software, serving the purpose of alerting the pilot if current flight is being conducted in the critical onset period, which takes place for 3.5 minute until the propulsion system is no longer able to sustain flight. The identification of this period is absolutely critical since it allows the pilot to make an educated, quantified decision of whether to land immediately or continue with the mission based on what's best for mission score.

## 8.2 Demonstrated Flight Performance of Aircraft

Many test flights have been executed to validate the performance of the aircraft. The flights that resulted in the most notable changes have been summarized in table 8.2.1 along with changes made to improve flight performance.

Flight	Date	Objectives	Outcomes
1	11/11/18	- First flight test on ramp - Determine if aircraft can takeoff based on DTS_Cat predictions	- Takeoff was successful - Unstable flight dynamics due to improper thrust angle
2	11/17/18	- Test and insure landing gear and forward/backward tip dynamics are adequate - Test radome aerodynamic influences	- Unstable landing gear causing forward tip - Undesirable wingtip stall at 35 ft/s
3	11/18/18	- Test modified wing geometry - Test stall characteristics	- Radome posed no significant change to flight characteristics - Undesirable wingtip stall at 35 ft/s
4	12/18/18	- Further test stall characteristics	- Stall speed was brought down to 24 ft/s - Wingtip stall was addressed
5	1/15/19	- Test propulsion system adequacy for six attack stores	- Successful takeoff, adequate performance
6	2/14/19	- Test $M_1 - M_3$ performance with full payload	- Adequate, however aircraft overshot turns in 25 MPH winds
7	2/30/2019	- Test third prototype with improved flight dynamics	
8	3/10/2019	- Test final aircraft for further incremental changes	

Table 8.2.1: Flight Design Validation and Outcomes

The 2/14/19 test was the most comprehensive test up to the date of this report. Flight performance and comparison with theoretical designed parameters are summarized in table 8.2.2 for each flight mission. All flights have been conducted in accordance with the model defined in section 4.4, Mission Model. Furthermore, the flight took place in 25 MPH winds, 10 MPH more than what is expected to take place in Arizona.

Performance Validation	Data	Predicted	Flown
M <sub>1</sub>	Flight Speed	80 ft/s	73 ft/s
	Current	10 A	8 A
M <sub>2</sub>	Flight Speed	100 ft/s	93 ft/s
	Lap Time	42.45 s	55.39 s
M <sub>3</sub>	Current	17 A	18 A
	Flight Speed	65-100 ft/s	65-93 ft/s
	Lap Time <sub>avg</sub>	42.89 s	64.56 s
	Attack Stores Launched	~15 A <sub>avg</sub>	~17 A <sub>avg</sub>

Table 8.2.2: Actual Flight Mission Performance in 25 MPH Winds

As seen in table 8.2.2, the aircraft struggles to meet the requirements for all missions, as expected, due to 25 MPH winds that are present. The Mission Model assumed a constant 15 MPH headwind, leading to the discrepancies acquired in the validation test. This indicates that further aerodynamic optimization must take place to allow the aircraft to perform better in high wind speeds. Further testing took place by analyzing the aircraft's ability to quickly react to the pilots input during flight in high wind speed situations, presented in figure 8.2.1. Note, due to telemetry data discontinuity during the 360 degree turn, it was filtered out of the data. Due to weather conditions, the team was unable to attempt the test flight mission to recapture the data, however the time duration of flight was still accurately captured.



Figure 8.2.1: Flight Mission Path Deviation

At 25 MPH winds, it was evident that turns with the wind resulted in the aircraft's inability to execute pilot input adequately. This caused an overshoot with respect to the way-point of the pilot. Against the wind vector, the pilot is able to better execute sharp turns as expected. Further analysis must take place to accurately optimize flight control surfaces, giving the pilot more authority to execute turns in high wind conditions. Overall, the team was pleased to see the plane perform this well, and looks forward to continually improving flight dynamics and performing test with the full propulsion system intact.

## References

- [1] [https://www.mathworks.com/products/matlab.html?s\\_tid=hp\\_products\\_matlab](https://www.mathworks.com/products/matlab.html?s_tid=hp_products_matlab)
- [2] Aerospaceweb.org, *Aircraft Landing Gear Layouts*, September 2004  
Available at: <http://www.aerospaceweb.org/question/design/q0200.shtml>  
2/10/2018, 18:56
- [3] Akanksha Dadhich & Dishant Kothia & Japneet Singh, *Design, Analysis, and Optimization of Folding Wing Mechanisms for Effective Utilization of Air Side Area*, Sept. 2016, International Journal of Aerospace and Mechanical Engineering
- [4] Jamey D. Jacob & Suzanne W. Smith, *Design Limitations of Deployable Wings for Small Low Altitude UAVs*, Jan. 2009, AIAA Aerospace Sciences Meeting
- [5] <http://ardupilot.org/copter/docs/common-pixhawk-overview.html>